The change in conductivity anisotropy due to superconductivity onset in the form of rare isolated islands: the theory and its application to FeSe

Pavel D. Grigoriev,
Landau Institute for Theoretical Physics, Russia

We find and quantitatively describe a general property: if superconductivity in an anisotropic conductor first appears in the form of isolated superconducting islands, it reduces electric resistivity anisotropically with maximal effect along the least conducting axis. This gives a simple tool to study inhomogeneous superconductivity in various anisotropic compounds and to estimate the volume fraction of superconducting phase, which helps to investigate the onset of high-temperature superconductivity. Using this property and the measurements of electron conductivity and diamagnetism, we show the appearance of inhomogeneous superconductivity in a bulk compound FeSe at ambient pressure and temperature 5 times higher than Tc = 8K, corresponding to zero resistance. This discovery helps to understand the many unusual superconducting properties of FeSe, such as a fivefold increase in Tc with increasing pressure to several kbars. The application of this property to detect spatially inhomogeneous superconductivity in other anisotropic compounds, such as cuprates and organic metals, is discussed.

A.A. Sinchenko, PG et al., Phys.Rev. B 95,165120 (2017);
PG et al., JETP Lett. 105 (12), 786 (2017)

General properties of $FeSe$ ($FeSe_{0.98}$)

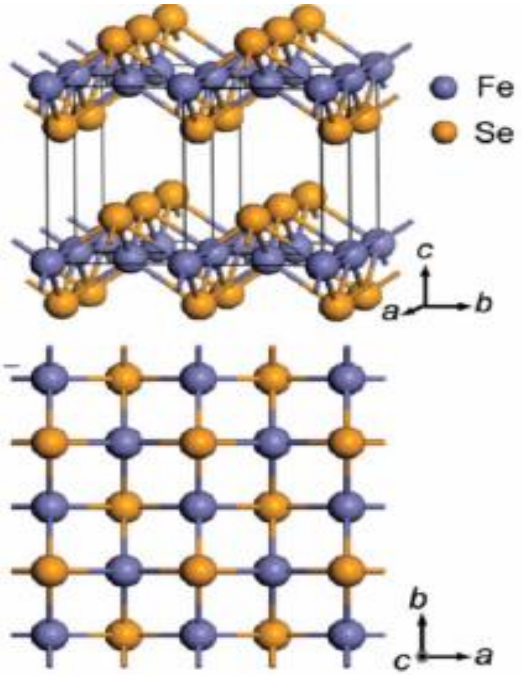

Simplest crystal structure of all Fe-based superconductors. At T≈ 90 K a structural (nematic) transition from tetragonal to orthorombic phase without magnetic order.

5-times increase of T_c under pressure (**Medvedev et al., Nat. Mater. 8, 630 (2009)**) and **static magnetic ordering** (M. Bendele et al., J Supercond Nov Magn 27, 965 (2014)).

Anomalously high T_c (> 100 K) in monolayer films $FeSe/SrTiO_3$ (Ge, J.-F. et al. Nat. Mater. 14, 285 (2015).

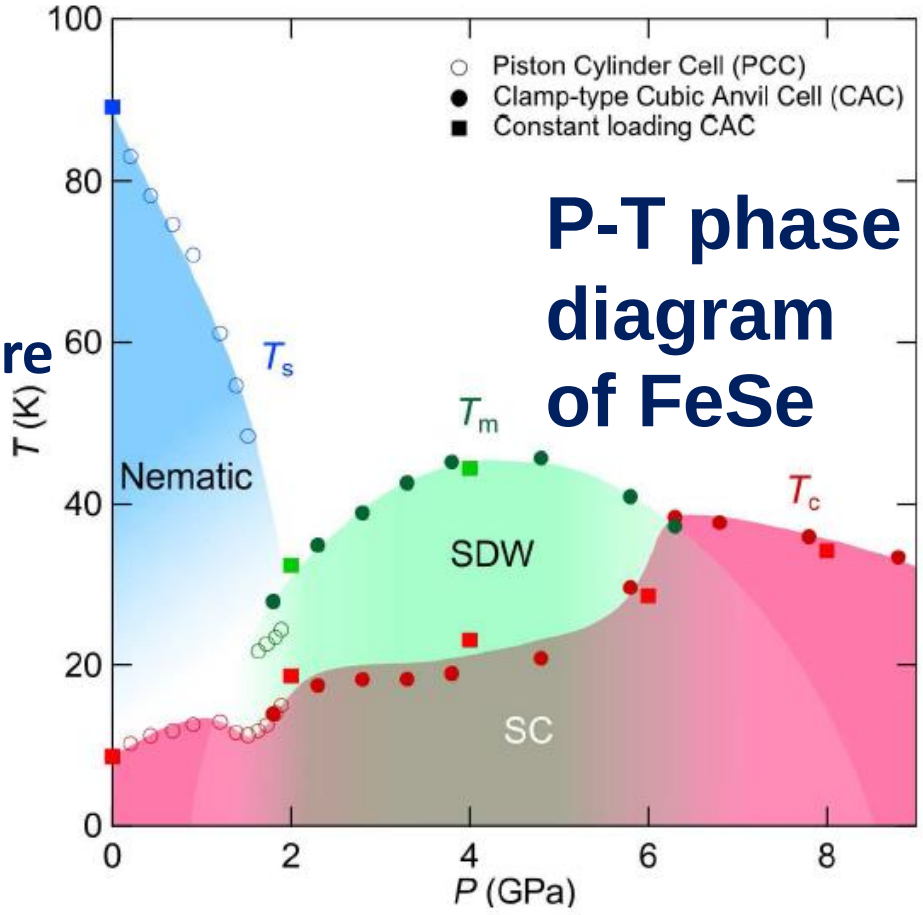

FeSe phase diagram (dependence on electron density)

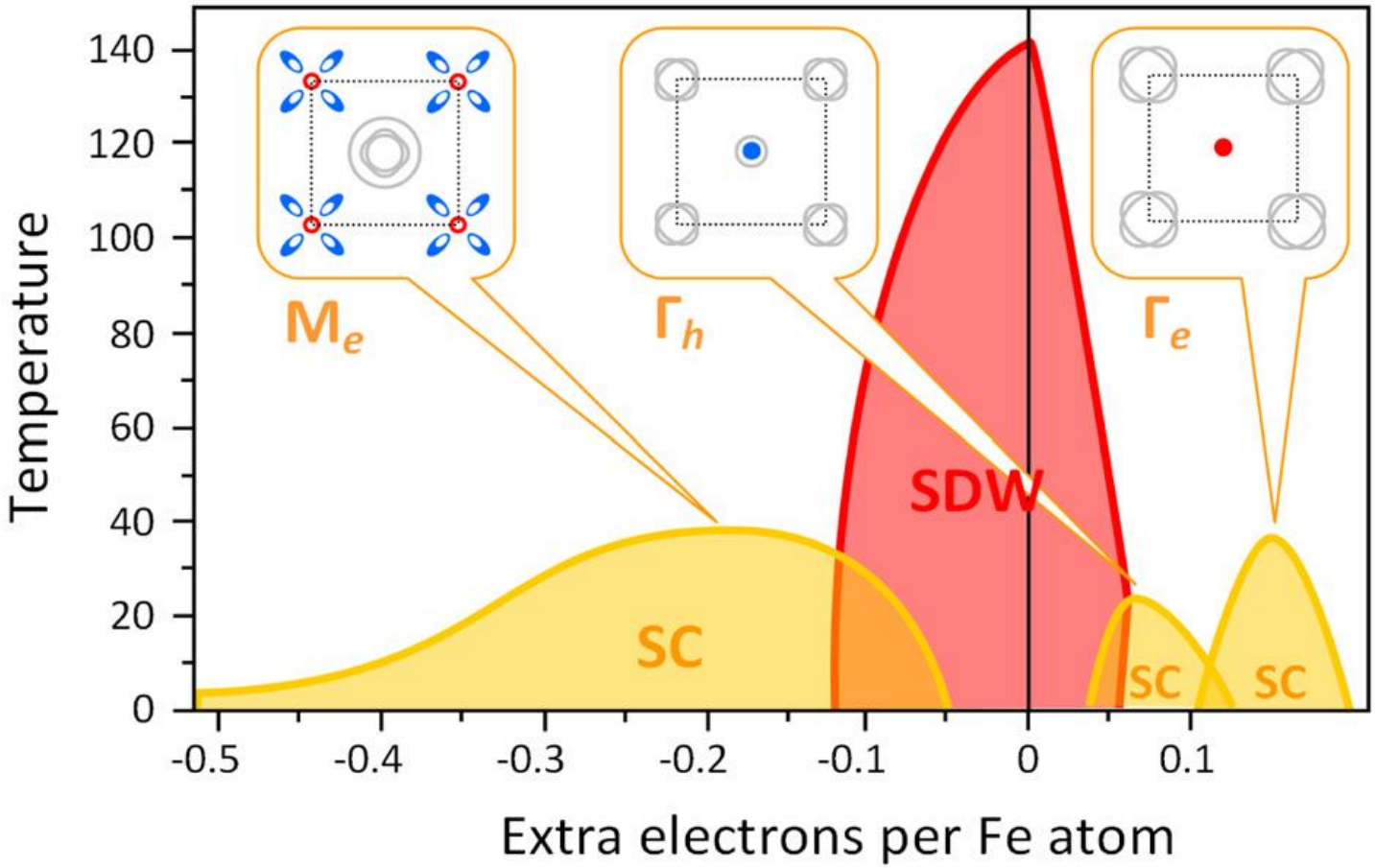

3 superconducting domes that can be classified by a proximity of the corresponding Van Hove singularity to the Fermi level: M_e, Γ_h, and Γ_e correspond to proximity to Lifshitz transition of the electron band in M-point and hole and electron bands in Γ point, respectively.

Experiment (A.A. Sinchenko et al.)

Two types of structures, prepared from FeSe monocrystals by FIB:

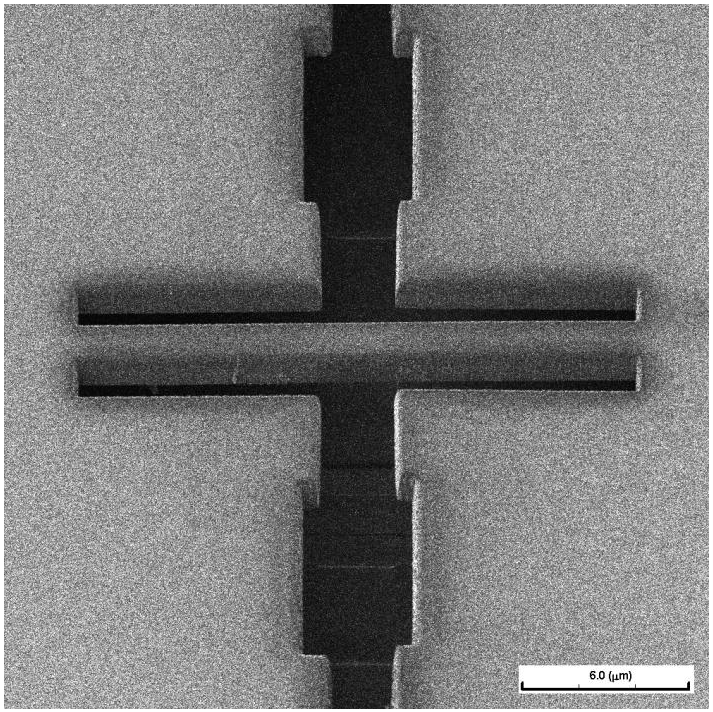

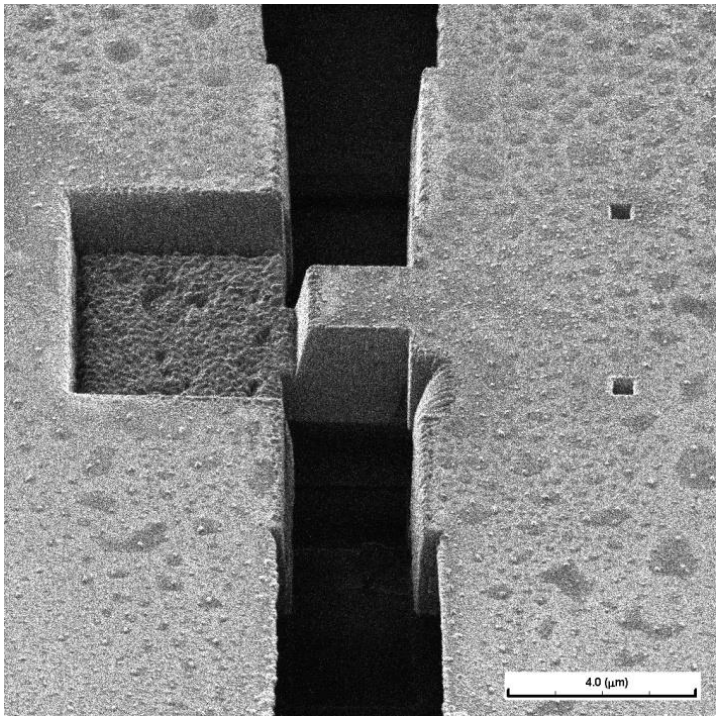

Structure A:

Microbridge in the (ab) plane

Size: 20 x 2 x (2-4) µm

Measures in-plane conductivity

Structure B:

Microbridge ⊥ (a-b) plane (along c-axis). Size: 0.2 x 2 x 2 µm

Measures out-of-plane conductivity

Experimental results: comparison of excess conductivity || and ⊥ conducting layers

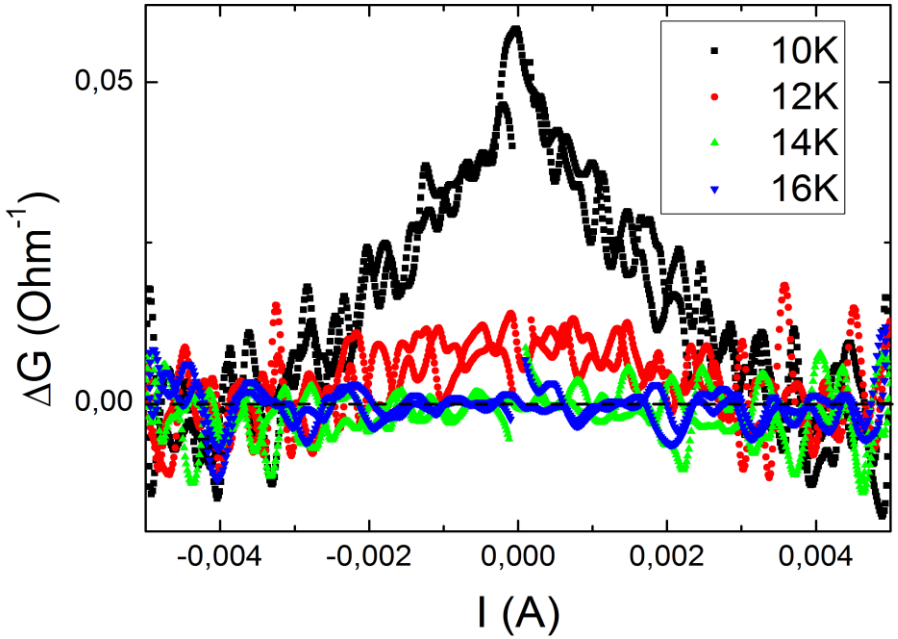

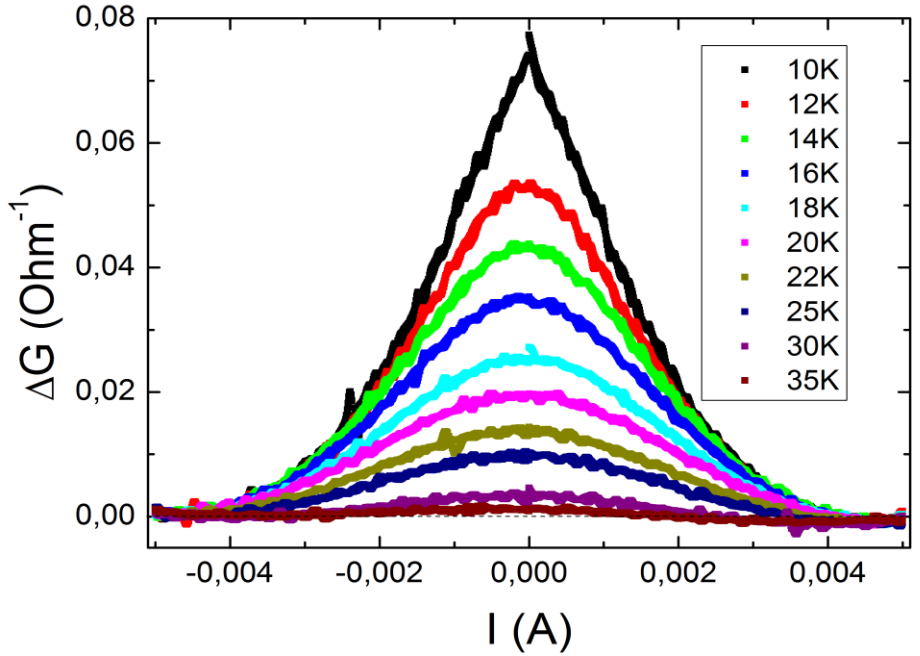

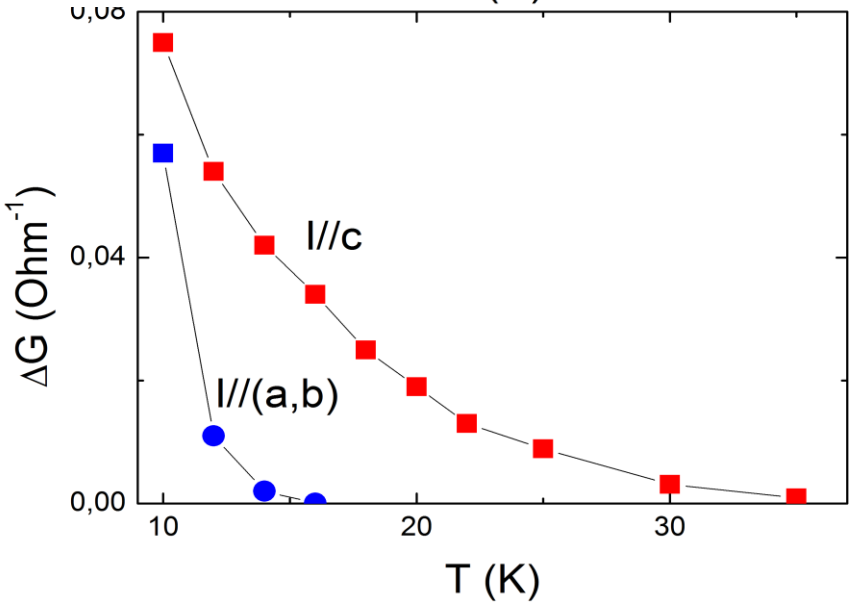

Excess conductivity ⊥ layers is greater and survives at higher T

The traces of superconducting transition are seen up to T ≈ 40K, as Tc under pressure ~ 6GPa or at doping.

Additional argument for superconductivity in FeSe – diamagnetic susceptibility

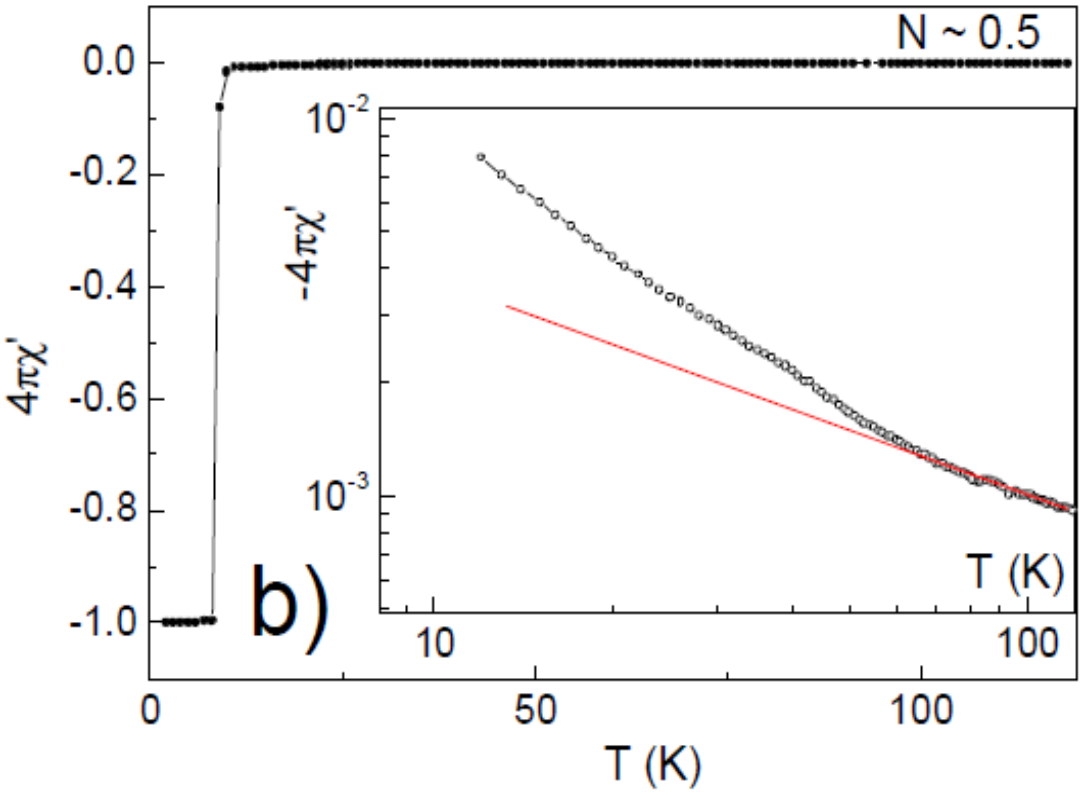

The temperature dependence of real part of magnetic susceptibility of FeSe single crystal. Main panel contains initial $4\pi\chi$ curve obtained for demagnetizing factor N~0.5, and the inset represents the same curve in double logarithmic scale to highlight the negative deviation at high temperatures. The red line is a guide for an eye.

Similar behavior in organic metals

PHYSICAL REVIEW B 81, 100509(R) (2010)

Domain walls at the spin-density-wave endpoint of the organic superconductor $(TMTSF)_2PF_6$ under pressure

N. Kang,[1] B. Salameh,[1,2] P. Auban-Senzier,[1] D. Jérome,[1] C. R. Pasquier,[1] and S. Brazovskii[3]

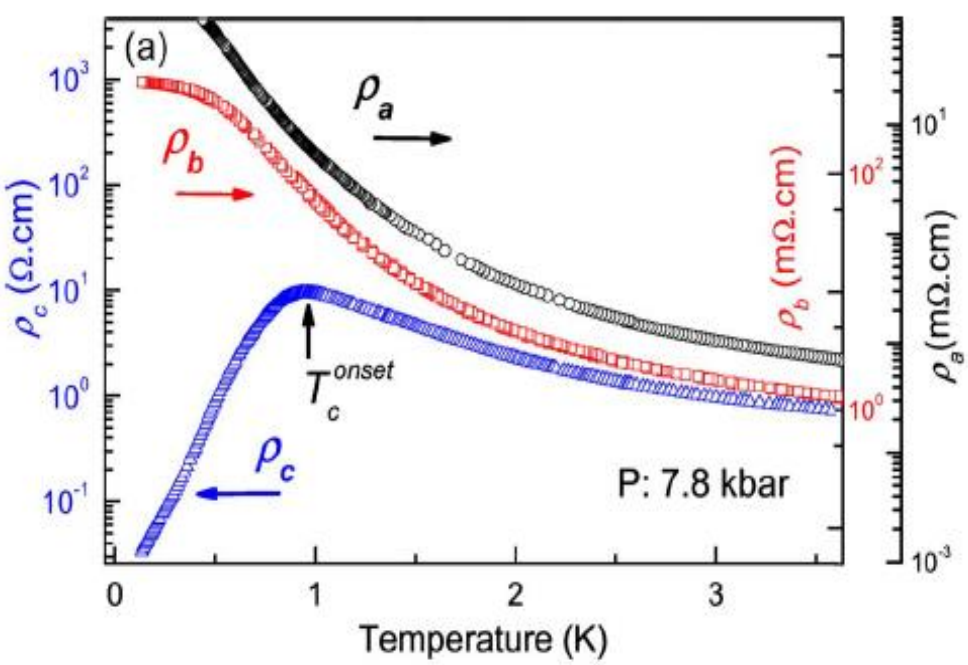

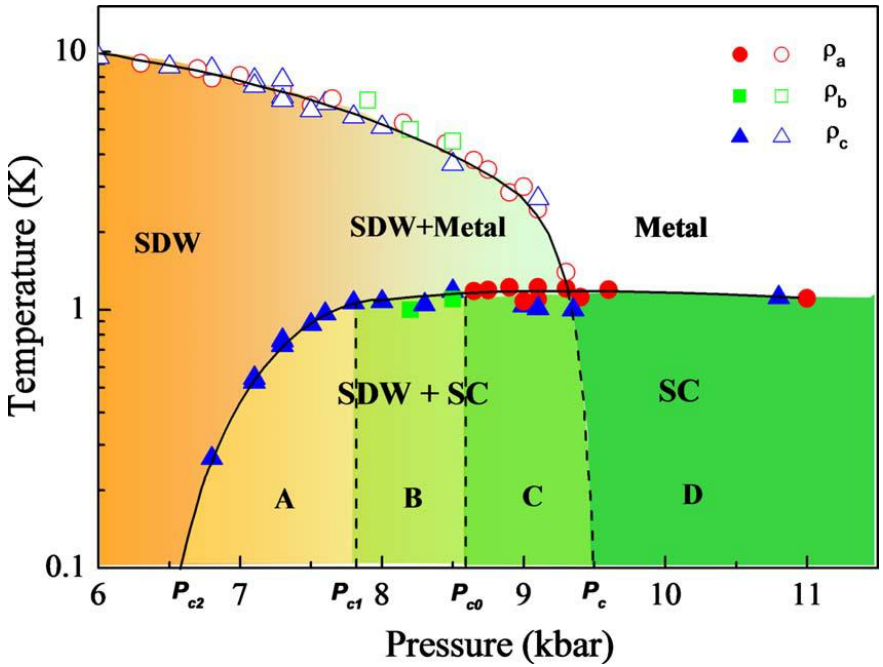

"the existence of one-dimensional and two-dimensional 2D metallic domains with a crossover from a filamentary superconductivity mostly along the *c axis to a 2D superconductivity in the* bc-plane perpendicular to the most conducting direction. The formation of these domain walls may be related to the proposal of a soliton phase in the vicinity of the critical pressure of the $(TMTSF)_2PF_6$ phase diagram."

FeSe – the same physical effect ???

Similar behavior in YBCO high-Tc superconductors?

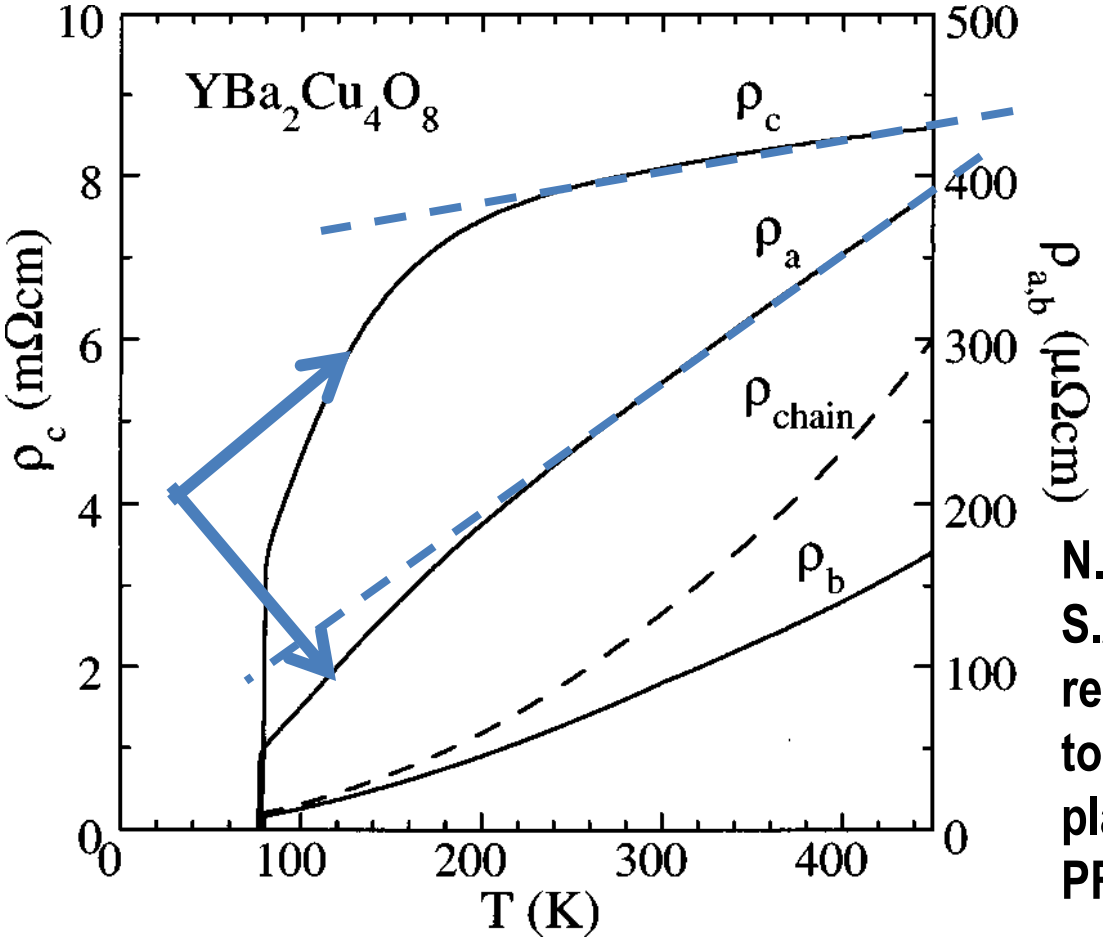

Resistivity along the c-axis (interlayer direction) starts to decrease at T≈200K

N.E.Hussey, K.Nozawa, H.Takagi, S.Adachi and K.Tanabe, "Anisotropic resistivity of $YBa_2Cu_4O_8$: Incoherent-to-metallic crossover in the out-of-plane transport" , PRB 56, R11 423 (1997)

Problem: What is the origin of anisotropic effect of superconductivity on conductivity?

Assume that superconductivity first appears in the form of isolated superconducting islands (or fluctuations). Why these superconducting islands reduce the interlayer resistivity much stronger than intralayer?

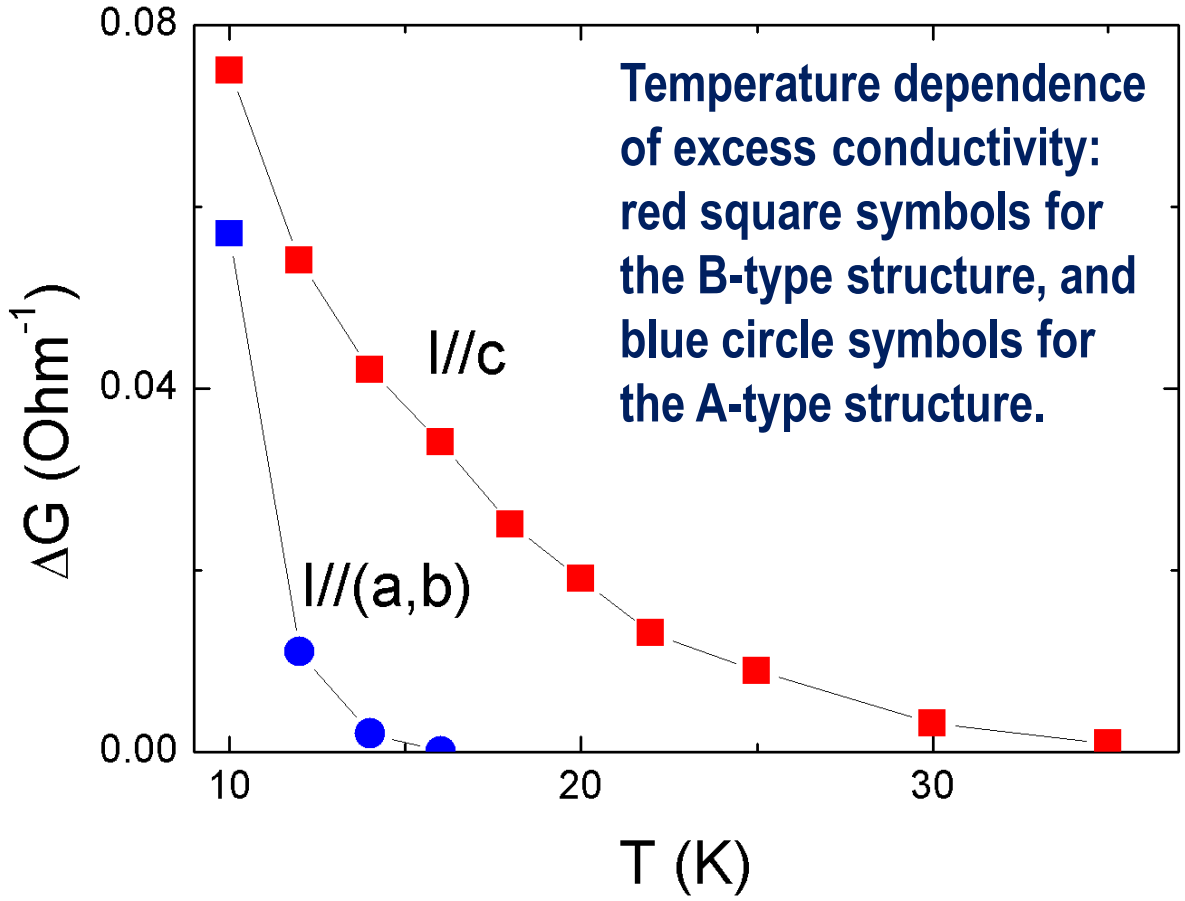

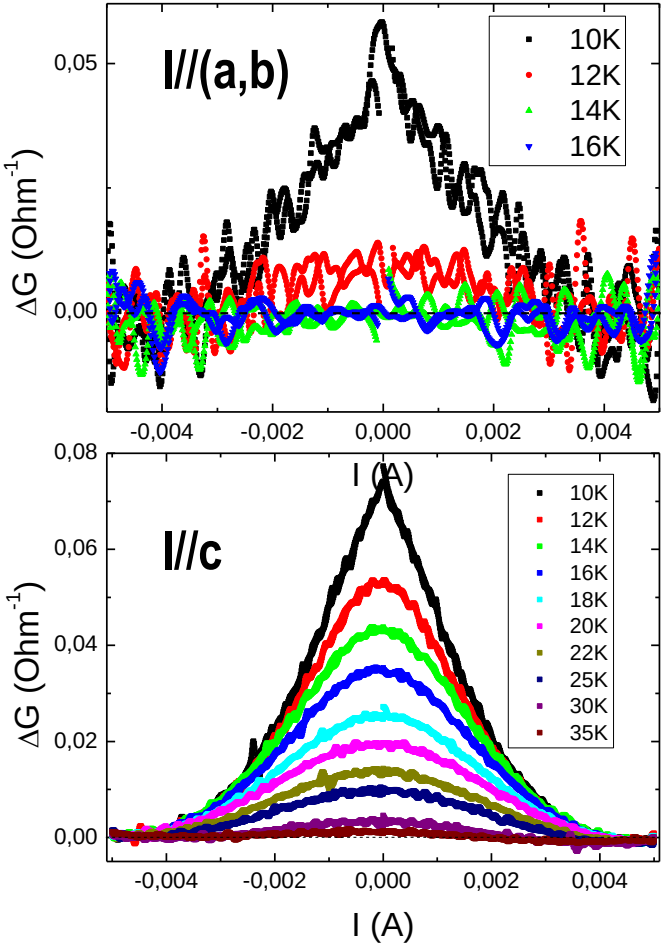

Fluctuations of superconductivity cannot explain such strong anisotropy of excess conductivity

Eqs. (3.34) and (3.35) of Varlamov&Larkin "Theory of fluctuations in superconductors", developed for Q2D electron dispersion $\varepsilon(k)=\varepsilon_{||}(k_{||})+2t_z\cos(k_z s)$, $t_z \ll E_F$, give

for the paraconductivity (excess conductivity along the intralayer and interlayer directions):

$$\sigma^{xx}(\epsilon,\, h\to 0,\, \omega=0)=\frac{e^2}{16s}\frac{1}{\sqrt{[\epsilon(r+\epsilon)]}},$$

$$\sigma^{zz}(\epsilon,\, h\to 0,\, \omega=0)=\frac{e^2 s}{32\xi_{xy}^2}\left(\frac{\epsilon+r/2}{[\epsilon(\epsilon+r)]^{1/2}}-1\right)$$

where $r=\frac{2\mathcal{J}}{\alpha T}=\frac{4\xi_z^2(0)}{s^2}$, $\epsilon=\ln\frac{T}{T_c}\approx\frac{T-T_c}{T_c}\ll 1$, s – interlayer distance.

At $\varepsilon \ll r$ this gives $\Delta\sigma_{zz}\approx\frac{e^2 s}{16\xi_{xy}^2}\frac{\xi_z^2(0)/s^2}{\sqrt{\epsilon(\epsilon+r)}}=\Delta\sigma_{xx}\frac{\xi_z^2(0)}{\xi_{xy}^2}\approx(\sigma_{zz}/\sigma_{xx})\Delta\sigma_{xx}$,

And at $\varepsilon \gg r$ this gives $\Delta\sigma_{zz}=\frac{e^2 s}{32\xi_{xy}^2}\left(\sqrt{\epsilon/(\epsilon+r)}-1\right)\ll\Delta\sigma_{xx}\frac{s^2}{\xi_{xy}^2}$,

i.e. the observed anisotropic excess of conductivity cannot be explained by the fluctuations at T<<Tc, because they give almost isotropic relative excess conductivity.

Qualitative explanation (of anisotropic effect of SC)

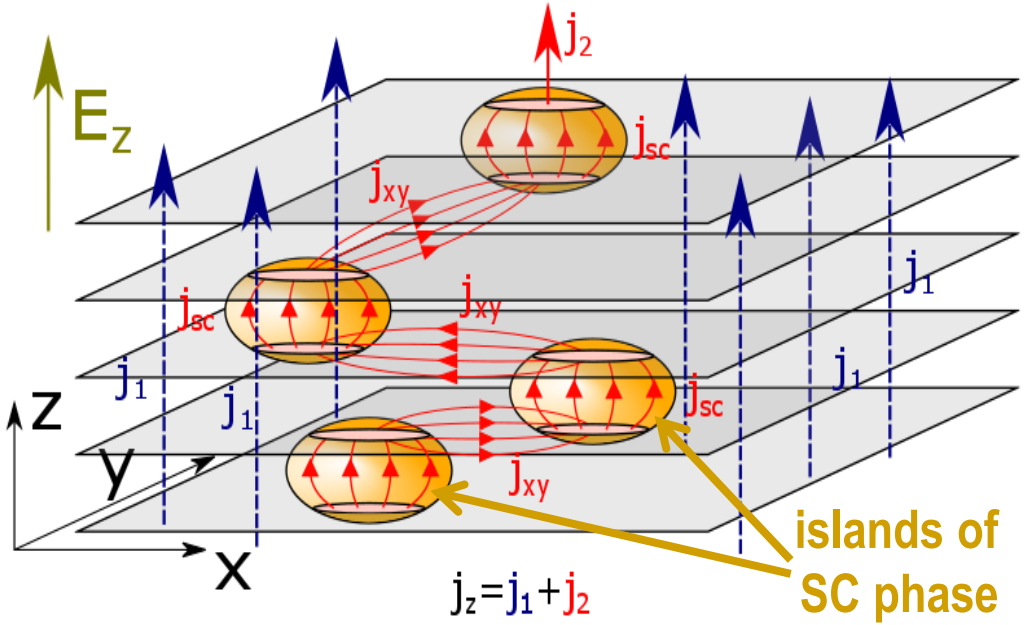

Result of our calculations confirms the qualitative idea:

$$\sigma_{zz} \approx \sigma_1 \left(\frac{\eta}{1-\phi} + \frac{\phi}{\ln\left(2/\sqrt{\eta}\right) - 1} \right)$$

$$\sigma_{xx} \approx \sigma_1 \left(1 + 2\phi\right)$$

$$\eta = \sigma_{zz}/\sigma_{xx} \ll 1$$

Two ways of interlayer current. The first way j_1 perpendicular to layers is slightly affected by superconductivity and contains the small anisotropic factor $\eta=\sigma_{zz}/\sigma_{xx}$. The rare superconducting inclusions then only slightly increase corresponding interlayer conductivity $\sigma_{zz}^{(1)}$ proportionally to their volume ratio ϕ. The second way j_2 is the diffusive path via superconducting islands. It has no local current density along the z-axis in the normal phase, and the interlayer conductivity $\sigma_{zz}^{(2)}$ does not acquire the small anisotropy factor η. However, its path along the conducting layers between rare superconducting islands is long and inversely proportional to the volume ratio ϕ of superconducting phase: $\sigma_{zz}^{(2)} \sim \phi\, \sigma_{xx}$. The total interlayer current j_z is approximately a sum of these two contribution.

Step 1: The model (rare isolated SC islands)

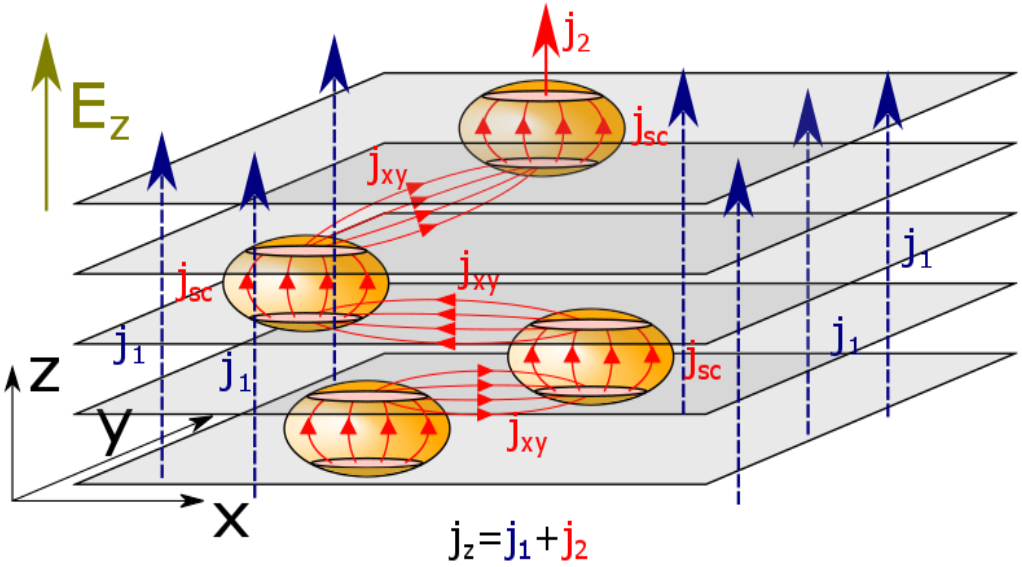

1.Effective conductivity in the Maxwell's (effective-medium) approximation for heterogeneous media with background isotropic conductivity σ_1 and spherical granules with conductivity $\sigma_2 \neq \sigma_1$ is given by the equation [Maxwell, 1873]:

$$\frac{\sigma_e - \sigma_1}{\sigma_e + 2\sigma_1} = \phi \frac{\sigma_2 - \sigma_1}{\sigma_2 + 2\sigma_1}$$

where ϕ is the total volume fraction of granules

In our model the background conductivity σ_1 is not isotropic and the granules with conductivity $\sigma_2 \neq \sigma_1$ are generally not spherical (may be spheroidal because of the anisotropy of SC coherence length).

But, as in the Maxwell's (effective-medium) approximation we assume that the concentration (volume fraction ϕ) of SC inclusions $\phi \ll 1$.

Step 2: mapping (dilatation) to isotropic problem

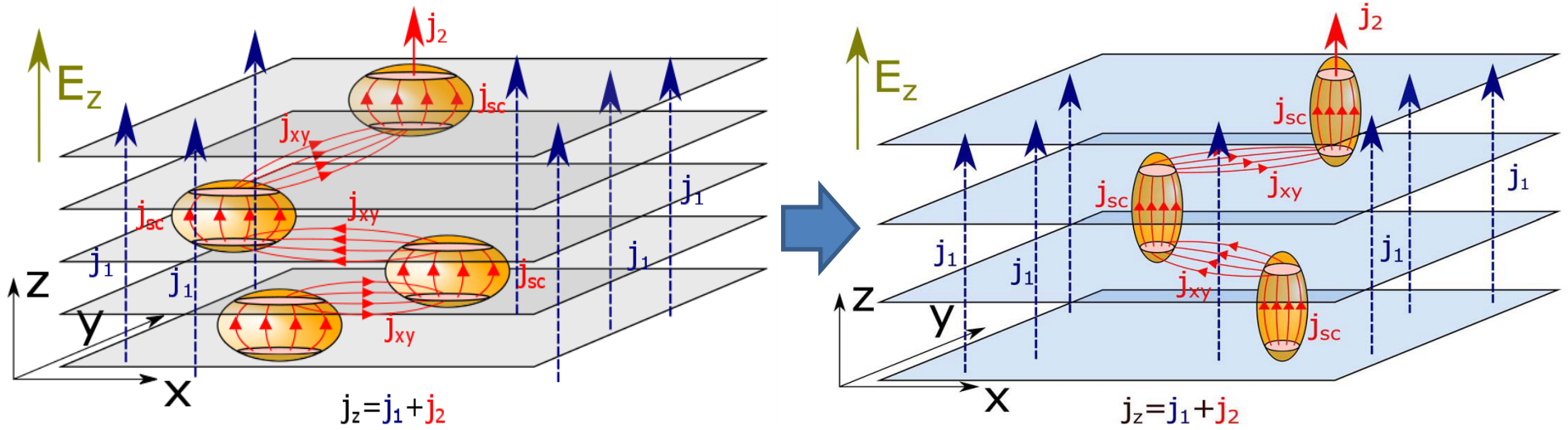

2. Next step - mapping of conductivity problem in anisotropic media to isotropic:

The electrostatic equation of continuity in Cartesian coordinates can be written as

$$-\nabla j = \sigma_{xx}\frac{\partial^2 V}{\partial x^2} + \sigma_{yy}\frac{\partial^2 V}{\partial y^2} + \sigma_{zz}\frac{\partial^2 V}{\partial z^2} = 0. \quad \eta \equiv \sigma_{zz}/\sigma_{xx} \ll 1$$

By the change of coordinates $x_* = x,\ y_* = \sqrt{\sigma_{yy}/\sigma_{xx}}\,y,\ z_* = \sqrt{\sigma_{zz}/\sigma_{xx}}\,z$

and by the simultaneous conductivity change: $\sigma^*_{zz} = \sigma^*_{yy} = \sigma^*_{xx} = \sigma_{xx}$

it transforms to the continuity equation for isotropic media:

$$-\nabla j = \sigma_{xx}\left(\frac{\partial^2 V}{\partial x_*^2} + \frac{\partial^2 V}{\partial y_*^2} + \frac{\partial^2 V}{\partial z_*^2}\right) = 0.$$

Calculation (1): first formulas

3. After the mapping, the spherical granules become ellipsoids. A generalization of the Maxwell approximation for a macroscopically anisotropic composite consisting of M-1 different types of unidirectionally aligned isotropic ellipsoidal inclusions of the same shape is given by [S.Torquato, ***Random Heterogeneous Materials***, Springer, 2001].

$$\sum_{j=1}^{M} \phi_j(\boldsymbol{\sigma}_e - \boldsymbol{\sigma}_j)\cdot \boldsymbol{R}^{(j1)} = 0 \quad \text{where } \boldsymbol{R}^{(j1)} = \left[\boldsymbol{I} + \boldsymbol{A}^* \frac{\sigma_j - \sigma_1}{\sigma_1}\right]^{-1}; \quad \boldsymbol{\sigma}_j = \sigma_j \boldsymbol{I}$$

and A* is the symmetric depolarization tensor of the d-dimensional ellipsoid, which in the principal axes frame has diagonal components or eigenvalues (denoted by A_j, i = 1, ... , d) given by the elliptic integrals: $$A_i^* = \left(\prod_{j=1}^{d} \frac{a_j}{2}\right) \int_0^\infty \frac{dt}{(t + a_i^2)\sqrt{\prod_{j=1}^{d}(t + a_j^2)}}$$

4. For a 3D spheroid, prolate (b>a) or oblate (b<a) $\chi_a^2 = -\chi_b^2 = (a^2/b^2) - 1$

$$\boldsymbol{A}^* = \begin{bmatrix} Q & 0 & 0 \\ 0 & Q & 0 \\ 0 & 0 & 1-2Q \end{bmatrix}, \text{ where } Q = \frac{1}{2}\left\{1 + \frac{1}{(b/a)^2 - 1}\left[1 - \frac{1}{2\chi_b}\ln\left(\frac{1+\chi_b}{1-\chi_b}\right)\right]\right\}, \ \frac{b}{a} \geq 1,$$

$$Q = \frac{1}{2}\left\{1 + \frac{1}{(b/a)^2 - 1}\left[1 - \frac{1}{\chi_a}\tan^{-1}(\chi_a)\right]\right\}, \ \frac{b}{a} \leq 1$$

If the SC islands were initially spherical, after the mapping $(a/b)^2 = \sigma_{zz}/\sigma_{xx} = \eta$, and $$2Q = 1 + \frac{1}{1/\eta - 1}\left[1 - \frac{1}{2\chi}\ln\left(\frac{1+\chi}{1-\chi}\right)\right]$$

Calculation (2): general result

5. In the new (mapped) geometry with isotropic σ_1 and spheroid superconducting islands with $\sigma_2 = 0$ the equation for diagonal components of the effective conductivity tensor σ_e^*

$$(1-\phi)\left(\boldsymbol{\sigma}_e^* - \sigma_1 \boldsymbol{I}\right) + \frac{\phi\left(\boldsymbol{\sigma}_e^* - \sigma_2 \boldsymbol{I}\right)}{\boldsymbol{I} + \boldsymbol{A}\left(\sigma_2 - \sigma_1\right)/\sigma_1} = 0, \quad \text{where}$$

$$\boldsymbol{A}^* = \begin{bmatrix} Q & 0 & 0 \\ 0 & Q & 0 \\ 0 & 0 & 1-2Q \end{bmatrix}, \qquad 2Q = 1 + \frac{1}{1/\eta - 1}\left[1 - \frac{1}{2\chi}\ln\left(\frac{1+\chi}{1-\chi}\right)\right]$$

and the eccentricity of SC spheroids $\chi = \sqrt{1-\eta}$

$$\eta \equiv \sigma_{zz}/\sigma_{xx} \ll 1$$

The solution of this equation is the diagonal matrix of the effective conductivity tensor σ_e^* in the mapped system:

$$\boldsymbol{\sigma}_e^* = \begin{pmatrix} \sigma_{xx}^* & 0 & 0 \\ 0 & \sigma_{yy}^* & 0 \\ 0 & 0 & \sigma_{zz}^* \end{pmatrix},$$

where for the volume ratio $\phi \ll 1$ of SC islands

$$\frac{\sigma_{xx}^*}{\sigma_1} = \frac{(1-Q)\,\sigma_1\,(1-\phi) + \sigma_2\,(Q+\phi-Q\phi)}{\sigma_1\,(1-Q\,(1-\phi)) + Q\sigma_2\,(1-\phi)}, \quad \sigma_{yy}^* = \sigma_{xx}^*, \text{ and}$$

$$\frac{\sigma_{zz}^*}{\sigma_1} = \frac{2Q\,(\sigma_2-\sigma_1)\,(1-\phi) - \sigma_2}{2Q\,(\sigma_2-\sigma_1)\,(1-\phi) - \sigma_2\,(1-\phi) - \phi\sigma_1}.$$

For SC islands $\sigma_2 = 0$.

This formally solves the problem (after mapping back), but the formulas are too long!

Calculation (3): simplification of the result

6. At $\sigma_2 \gg \sigma_1$ ($\sigma_2=\infty$) this simplifies to

$$\frac{\sigma_{xx}^*}{\sigma_1} \to \frac{Q(1-\phi)+\phi}{Q(1-\phi)} = 1 + \frac{\phi}{Q(1-\phi)}$$

$$\frac{\sigma_{zz}^*}{\sigma_1} \to \frac{2Q(1-\phi)-1}{(2Q-1)(1-\phi)} = \frac{1}{1-\phi} + \frac{2Q\phi}{(1-2Q)(1-\phi)}$$

7. For strong anisotropy $\eta = \sigma_{zz}/\sigma_{xx} \ll 1$, the eccentricity $\chi \approx 1 - \eta/2$, and we obtain

$$Q \approx 1/2 + \eta\left[1 + \ln(\eta/4)/2\right]/2\,, \qquad \sigma_{xx}^* \approx \sigma_1(1+2\phi)\,, \quad \text{and} \quad \frac{\sigma_{zz}^*}{\sigma_1} \approx \frac{1}{1-\phi} + \frac{\phi/\eta}{\ln\left(2/\sqrt{\eta}\right)-1}.$$

8. After the inverse mapping, back to initial geometry, $z = \sqrt{\eta} z_*$ and $\sigma_{zz} = \eta \sigma_{zz}^*$ we finally obtain

$$\sigma_{xx} \approx \sigma_1(1+2\phi)\,,$$

and

$$\sigma_{zz} \approx \sigma_1 \left(\frac{\eta}{1-\phi} + \frac{\phi}{\ln\left(2/\sqrt{\eta}\right)-1} \right)$$

Only slightly increases at small volume fraction ϕ of superconducting phase.

Contains two terms, corresponding to two ways of interlayer current. The first (standard) way contains small anisotropy factor η, and the second way contains small factor ϕ. At $\eta \ll \phi$ the second way gives the main contribution to the total interlayer conductivity.

Result for spheroidal superconducting inclusions

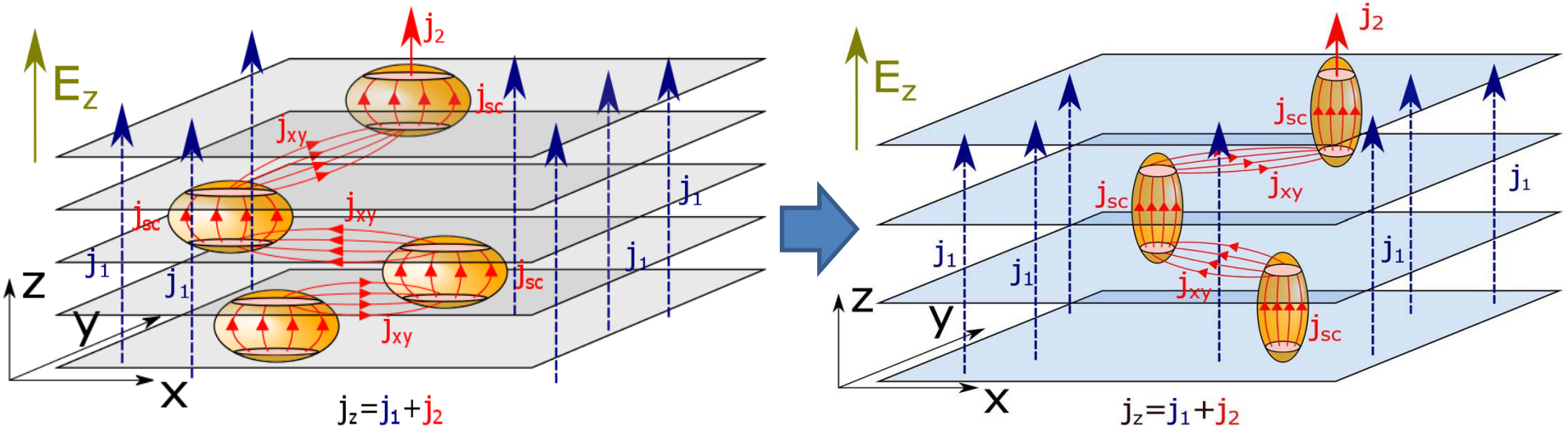

The initial ratio $\gamma=(a_z/a_x)^2$ is arbitrary. The final (after mapping) ratio $\gamma^*=(a_z^*/a_x^*)^2=\gamma/\eta>1$ because the parameter of the mapping (conductivity anisotropy) $\eta \equiv \sigma_{zz}/\sigma_{xx} \ll 1$

Finally, in the lowest order in φ, η, we obtain (after mapping back) the following expression for conductivity in heterogeneous media with spheroid superconducting inclusions

$$\frac{\sigma_{xx}}{\sigma_1} \approx \frac{1}{1-\varphi} + \varphi, \quad \frac{\sigma_{zz}}{\sigma_1} \approx \frac{\eta}{1-\varphi} + \frac{2\gamma\varphi}{\ln(4\gamma/\eta) - 2}.$$

where $\gamma=(a_z/a_x)^2$ is the initial ratio of main axes of spheroid superconducting islands, $\eta \equiv \sigma_{zz}/\sigma_{xx} \ll 1$ is anisotropy parameter, φ is volume fraction of SC phase

P. Grigoriev, A.A. Sinchenko et al., JETP Lett. 105 (12), 786 (2017)

Discussion of the result

We find and quantitatively describe a general property: if inhomogeneous superconductivity in a anisotropic conductor first appears in the form of isolated superconducting inclusions, it reduces electric resistivity anisotropically, with maximal effect along the least conducting axis.

For spherical islands of superconducting phase

$$\sigma_{xx} \approx \sigma_1 (1 + 2\phi) ,$$

Only slightly increases at small volume fraction ϕ of superconducting phase.

and

$$\frac{\sigma_{zz}}{\sigma_1} \approx \frac{\eta}{1-\varphi} + \frac{2\gamma\varphi}{\ln(4\gamma/\eta) - 2}.$$

Contains two terms, corresponding to two ways of interlayer current. The first (standard) way contains small anisotropy factor η, and the second way contains small factor ϕ. At $\eta \ll \phi$ the second way gives the main contribution to the total interlayer conductivity. This result agrees with proposed qualitative picture, and it allows to estimate the fraction of SC islands

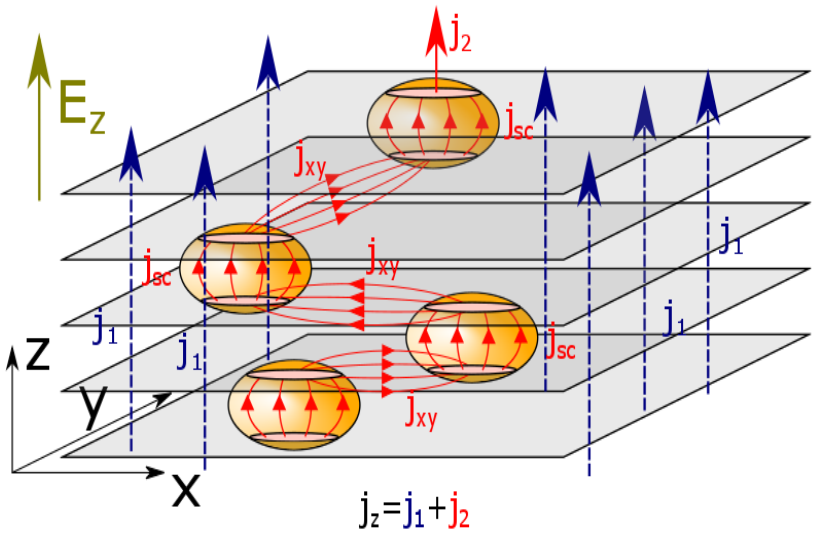

Additional argument for superconductivity in FeSe – diamagnetic susceptibility

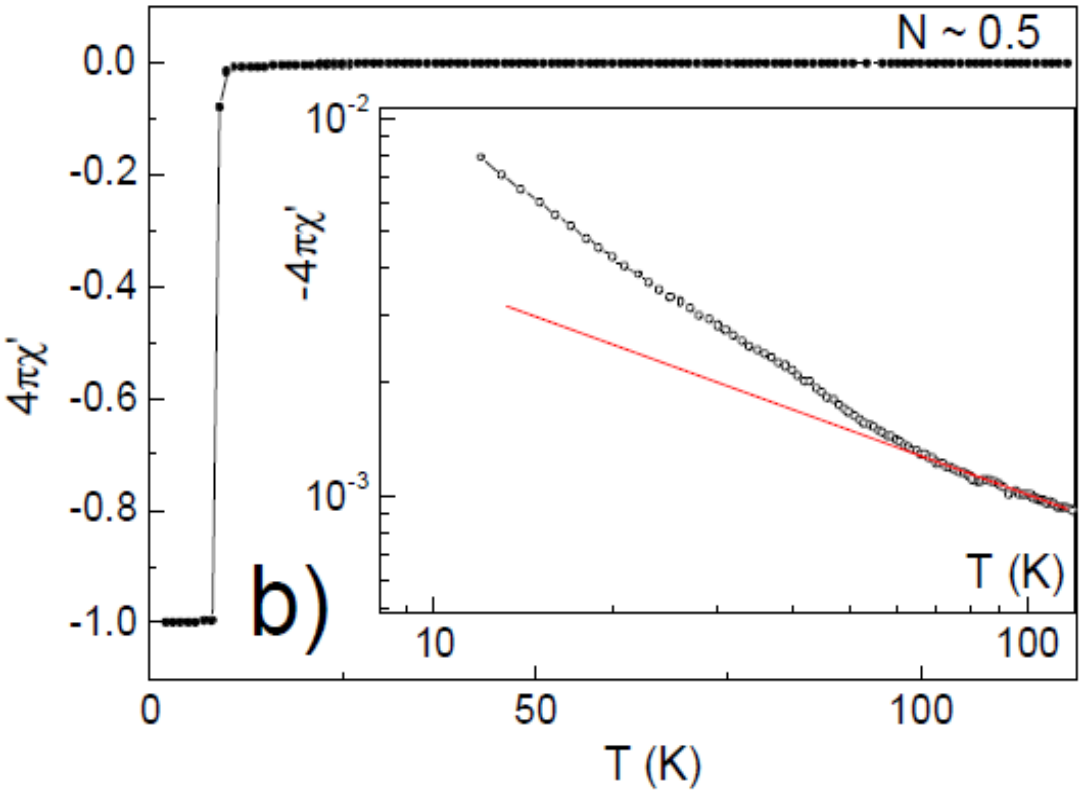

The temperature dependence of real part of magnetic susceptibility of FeSe single crystal. Main panel contains initial $4\pi\chi$ curve obtained for demagnetizing factor N~0.5, and the inset represents the same curve in double logarithmic scale to highlight the negative deviation at high temperatures. The red line is a guide for an eye.

Using the derived formulas one can compare the temperature dependence of the volume fraction ϕ of superconducting phase, obtained from the diamagnetic and conductivity measurements.

Comparison of the temperature dependence of the volume fraction $\phi(T)$ of superconducting phase, obtained from the diamagnetic susceptibility and conductivity measurements

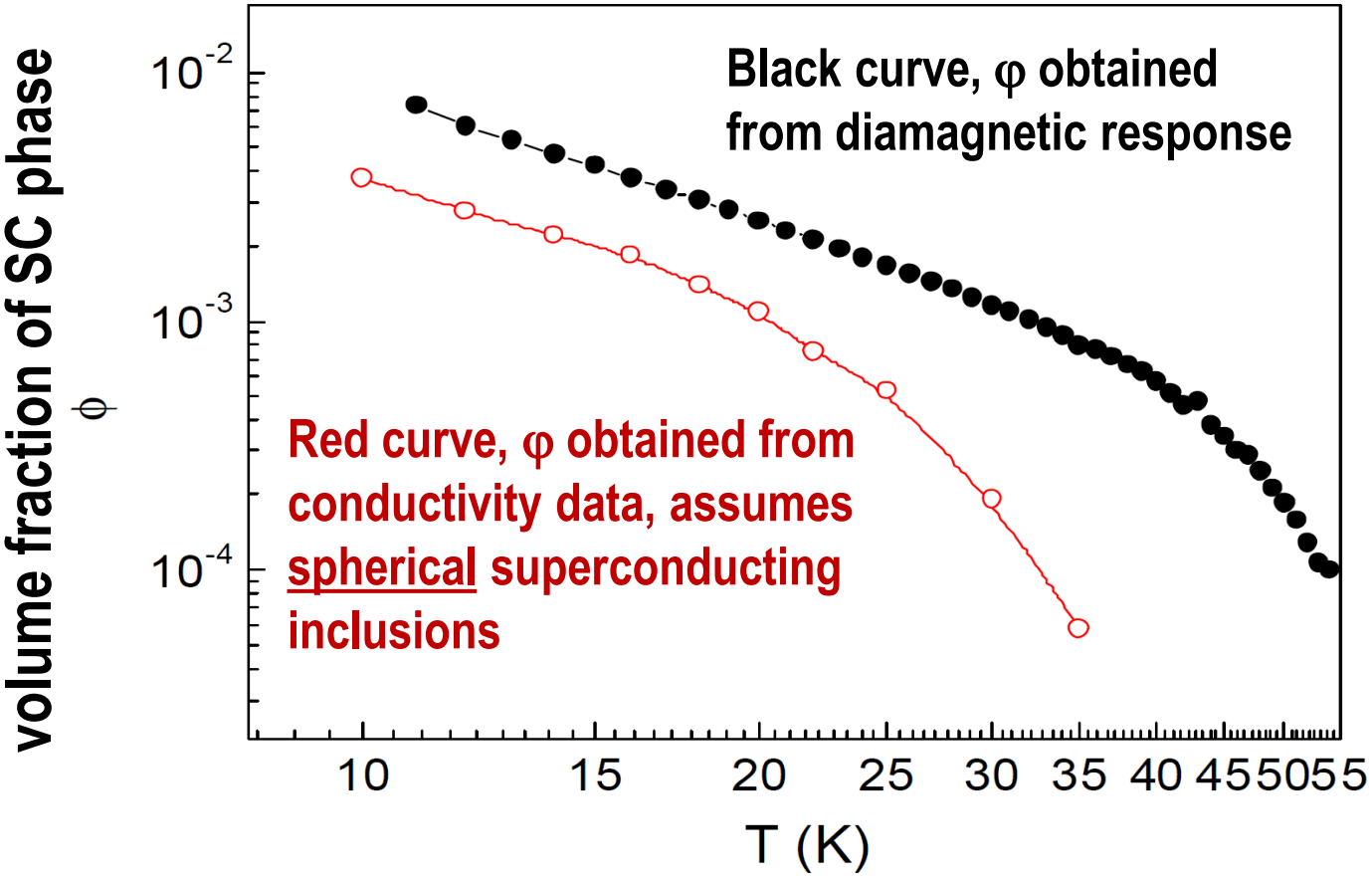

Conclusion: although qualitative agreement is obtained without any fitting parameters, for quantitative agreement one should take the shape of superconducting islands non-spherical but of oblate spheroids.

Comparison of the temperature dependence of the volume fraction $\phi(T)$ of superconducting phase, obtained from the diamagnetic susceptibility and conductivity measurements

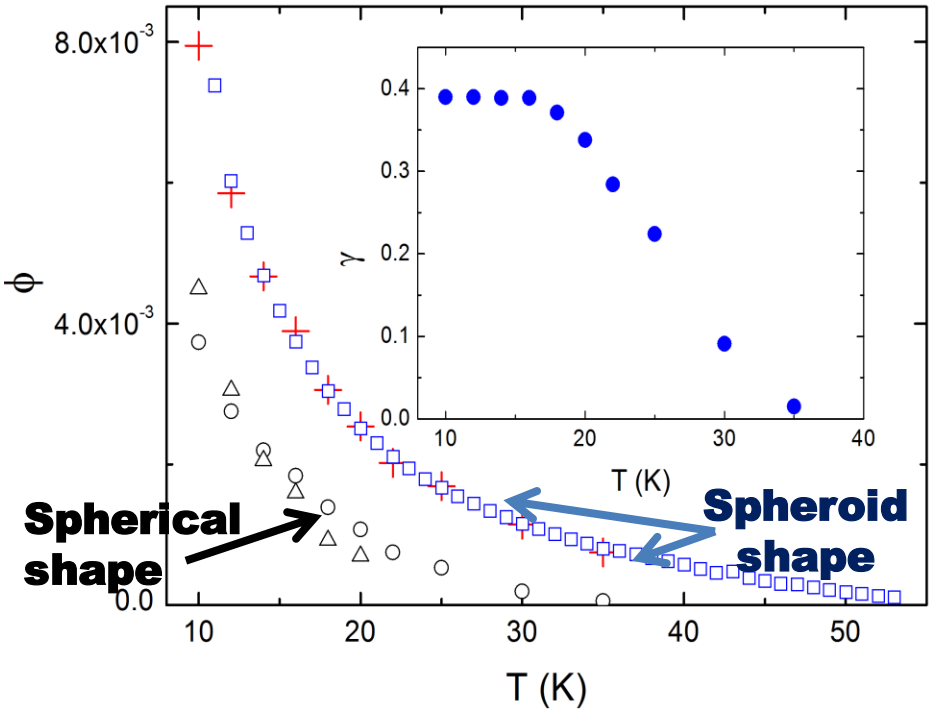

Temperature dependence of the volume fraction of the superconducting phase in FeSe. Circles and triangles correspond to the spherical shape of superconducting granules, squares are values obtained from magnetic measurements, and crosses are the values obtained from transport measurements for spheroid shape with the dependence $\gamma(T)$ shown in the insert.

$$\frac{\sigma_{xx}}{\sigma_1} \approx \frac{1}{1-\varphi} + \varphi, \quad \frac{\sigma_{zz}}{\sigma_1} \approx \frac{\eta}{1-\varphi} + \frac{2\gamma\varphi}{\ln(4\gamma/\eta) - 2}. \qquad \eta \equiv \sigma_{zz}/\sigma_{xx} \ll 1$$

One obtains a quantitative agreement at temperature T<20K if takes the shape of superconducting islands as oblate spheroids with axes ratio

$$a_z/a_x = 0.62$$

But for agreement at higher temperature one needs to take more oblate spheroids

Doubling of the critical temperature of FeSe observed in point contacts

PHYSICAL REVIEW B 93, 144515 (2016)

Yu. G. Naidyuk,[1,2] G. Fuchs,[2] D. A. Chareev,[3,4] and A. N. Vasiliev[4,5,6]

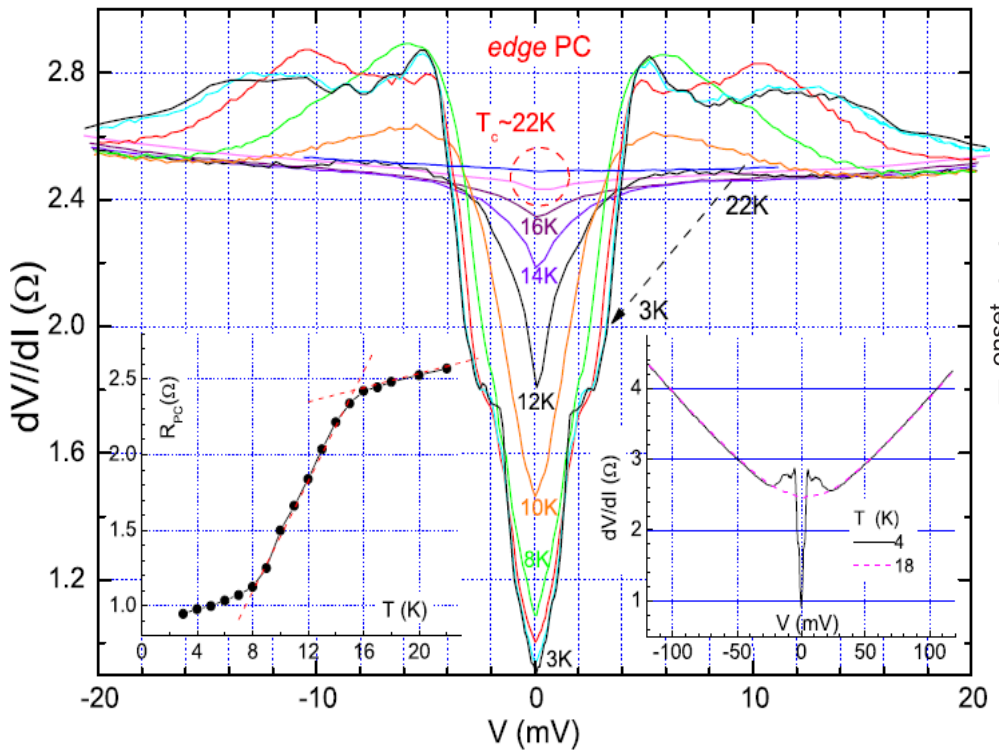

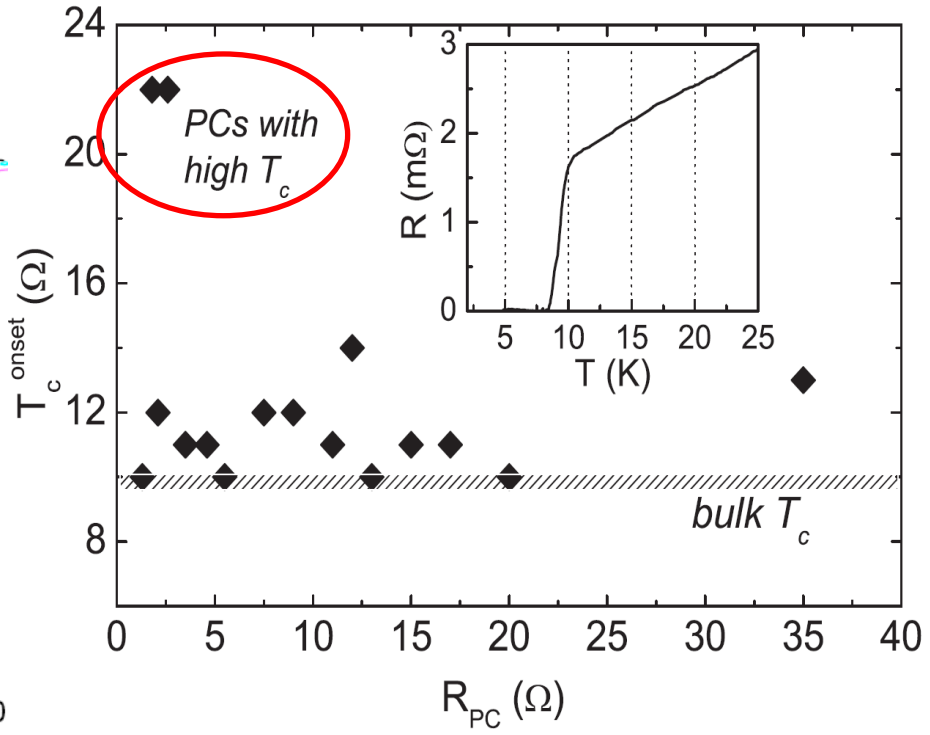

Evolution of *dV/dI* curves with temperature for a PC created by touching an edge of a FeSe crystal with a Cu wire. The upper two curves marked by the circle are measured at 18 and 22 K (top curve). The right inset shows two *dV/dI* curves measured at 4 and 18 K for a larger bias. The left inset shows the dependence of the PC resistance at zero bias versus temperature.

Statistic data for T_c^{onset} variation for point contacts with different resistances. Two PCs with high T_c are beyond the statistical error.

This supports inhomogeneous SC onset in FeSe

Spatial heterogeneities in Fe-based superconductors

PRL 112, 047005 (2014)

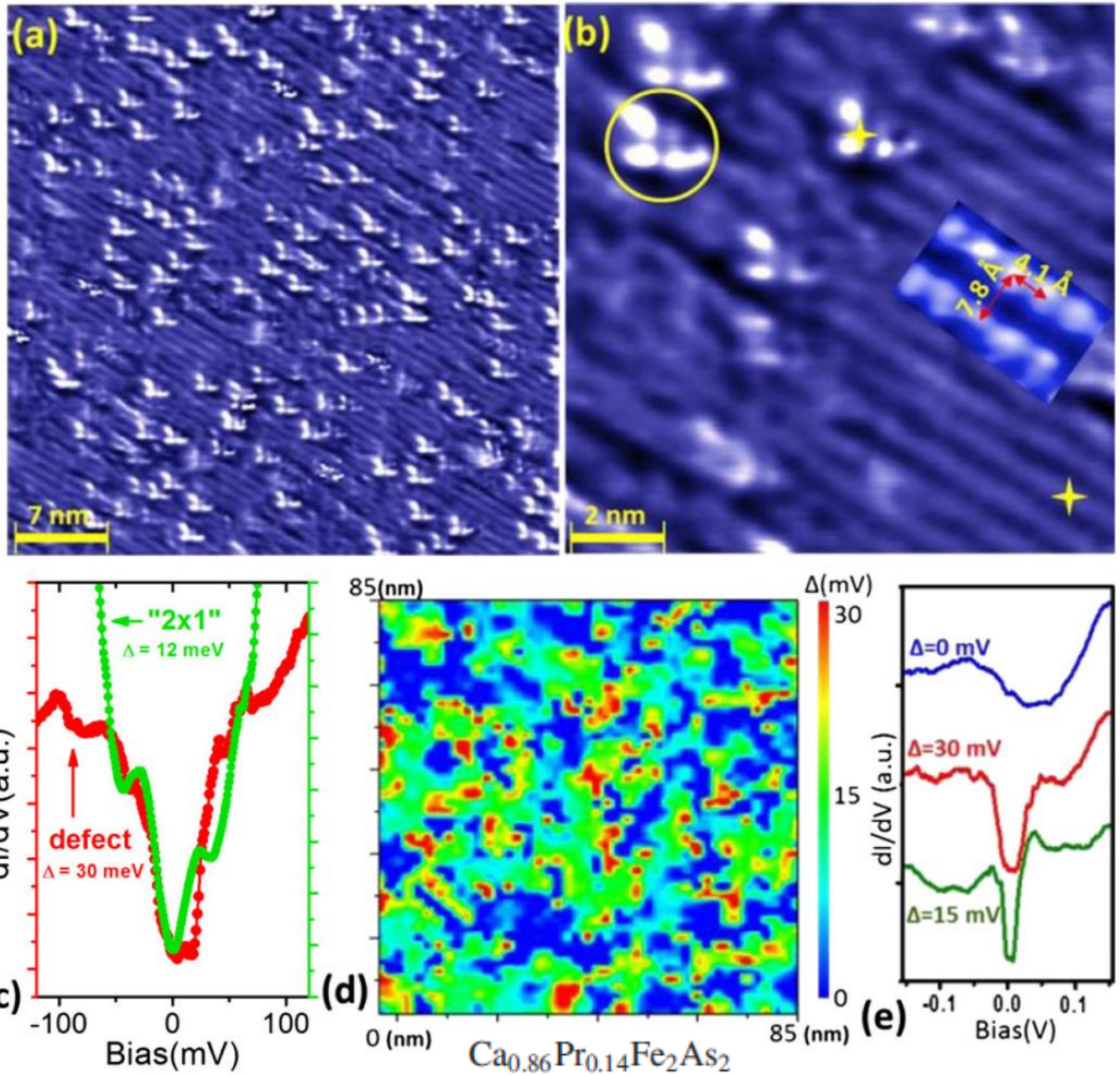

Spatial inhomogeneities in BISCCO [NATURE 413, 282 (2001)]

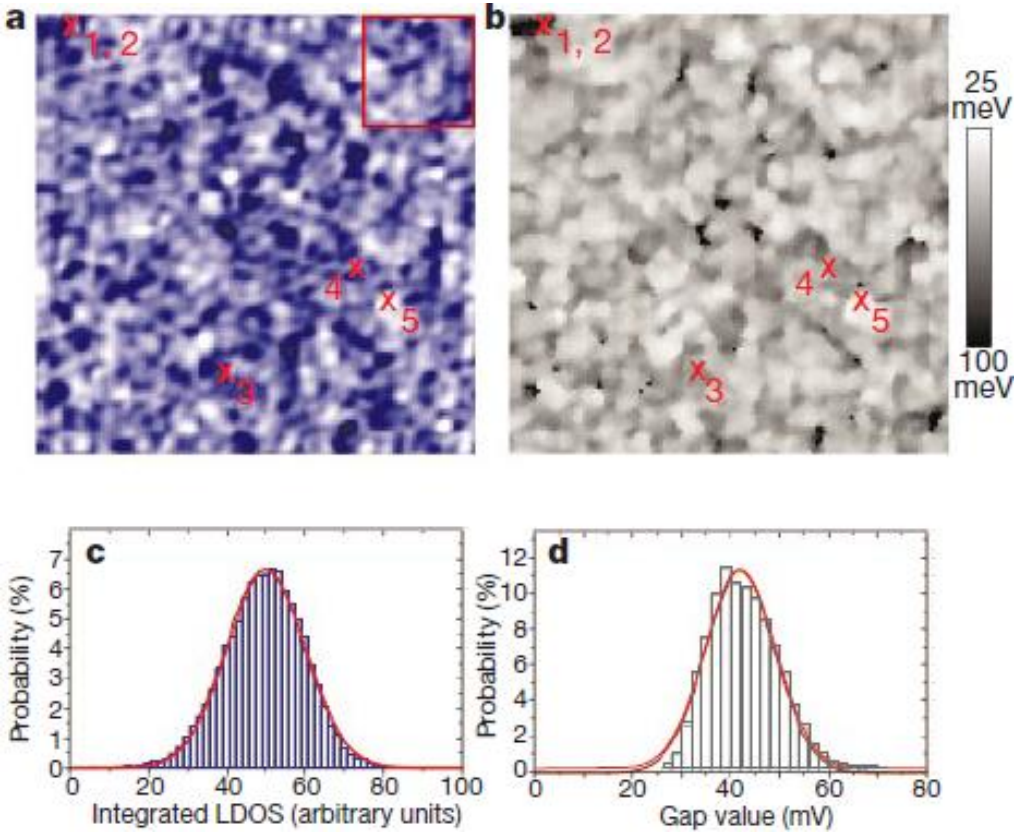

A LDOS map and superconducting gap map with their associated statistical results. a) 600x600A LDOS map obtained on a single crystal $Bi_2Sr_2CaCu_2O_{8+x}$ doped with a very dilute concentration (0.2%) of Zn atoms. The crystal has a superconducting transition temperature of 84 K, with a transition width of 4 K. It clearly displays an inhomogeneous structure. b) Superconducting gap map, obtained simultaneously with the integrated LDOS map on the same location, showing the spatial variation of the superconducting energy gap.

The local gap values are extracted from the corresponding local differential conductance spectra. c, d) show the statistical distributions of the integrated LDOS and the magnitude of the superconducting gap. Each of them exhibits a gaussian-like distribution (fitting function displayed in red). The fit of the gap distribution (42 meV mean; ~20 meV FWHM) shows it to be slightly skewed.

Inhomogeneity of charge-density-wave order and quenched disorder in a high-T_c superconductor $HgBa_2CuO_{4+y}$

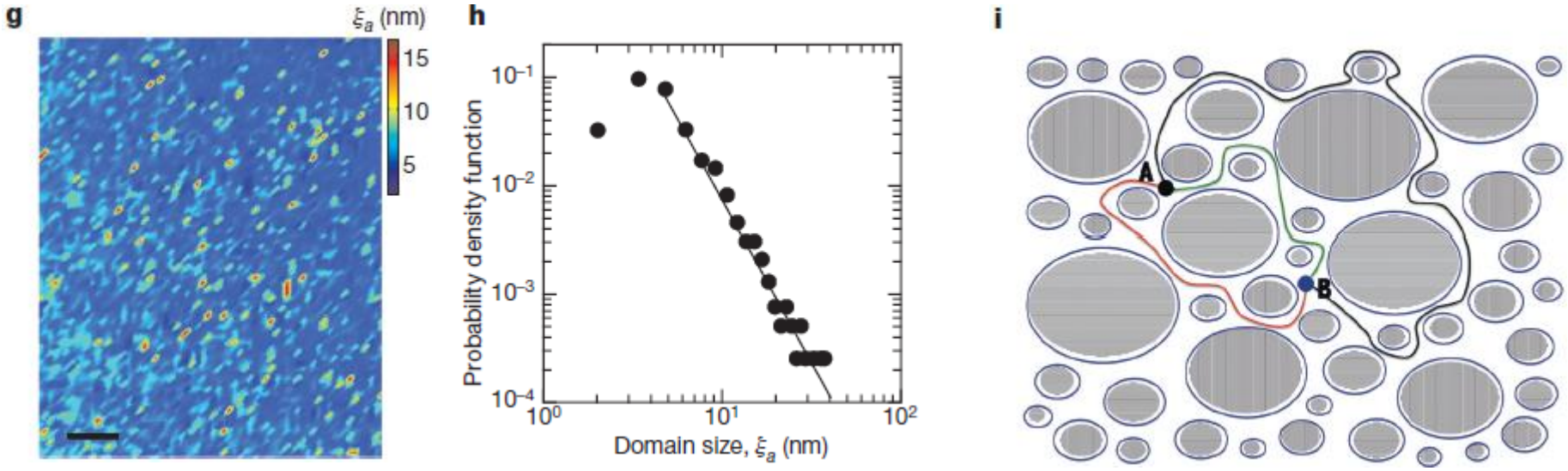

Spatial map (g) and probability density function (h) of the CDW-puddle size. Scale bar in g, 10mm. i, A schematic of non-equivalent paths for the superconducting current, running in the interface space between CDW puddles, connecting point A to point B.

[**G. Campi et al., Nature 525, 359–362 (2015)**]

Inhomogeneous superconductivity and the "pseudogap" state of novel superconductors

Vladimir Z. Kresin[a,*], Yurii N. Ovchinnikov[b], Stuart A. Wolf[c]

Physics Reports 431 (2006) 231–259

Many novel superconducting compounds such as the high T_c oxides are intrinsically inhomogeneous systems by virtue of the superconductivity being closely related to the carrier density which is in turn provided in most cases by doping. An inhomogeneous structure is thus created by the statistical nature of the distribution of dopants. At the same time doping also leads to pair-breaking and, consequently, to a local depression of T_c. This is a major factor leading to inhomogeneity. As a result, the critical temperature is spatially dependent: $T_c \equiv T_c(\mathbf{r})$.

The "pseudogap" state is characterized by several energy scales: T^*, T_c^*, and T_c . The highest energy scale (T^*) corresponds to phase separation (at $T < T^*$) into a mixed metallic-insulating structure. Especially interesting is the region $T_c^* > T > T_c$ where the compound contains superconducting "islands" embedded in a normal metallic matrix. As a result, the system is characterized by a normal conductance along with an energy gap structure, anomalous diamagnetism, unusual a.c. properties, an isotope effect, and a "giant" Josephson proximity effect. An energy gap may persist to temperatures above T_c^* caused by the presence of a charge density wave (CDW) or spin density wave (SDW) in the region $T > T_c^*$ but less than T^*, whereas below T_c^* superconducting pairing also makes a contribution to the energy gap (T_c^* is an "intrinsic" critical temperature). The values of T^*, T_c^*, T_c depend on the compound and the doping level. The transition at T_c into the dissipationless ($R = 0$) macroscopically coherent state is of a percolation nature.

Many experimental and theoretical papers argue a spatial separation of superconducting and normal/insulating phases in high-Tc cuprate superconductors, and the superconducting phase transition in isolated islands was proposed as an origin of pseudogap in cuprates. Whether the spatial inhomogeneity is a concomitant or assistant feature of high-temperature superconductivity is still debated, although various theoretical models propose an enhancement of superconducting transition temperature due to such inhomogeneity.

Therefore, the study of high-Tc superconductivity onset in the form of isolated islands is very important for understanding the cuprates.

Further work:

- consider quasi-1D anisotropy to describe organic metals and YBCO
- consider the arbitrary volume ratio ϕ of superconducting phase
- separate the contributions to the excess conductivity from spatial inhomogeneities (SC islands) and from SC fluctuations.

PHYSICAL REVIEW B 81, 100509(R) (2010)

Domain walls at the spin-density-wave endpoint of the organic superconductor $(TMTSF)_2PF_6$ under pressure

N. Kang,[1] B. Salameh,[1,2] P. Auban-Senzier,[1] D. Jérome,[1] C. R. Pasquier,[1] and S. Brazovskii[3]

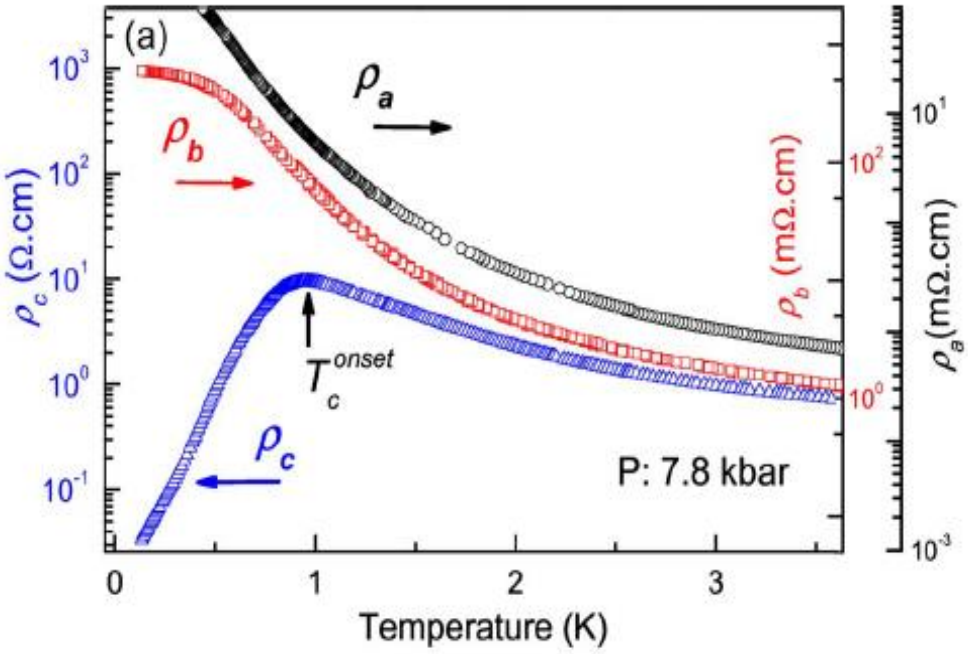

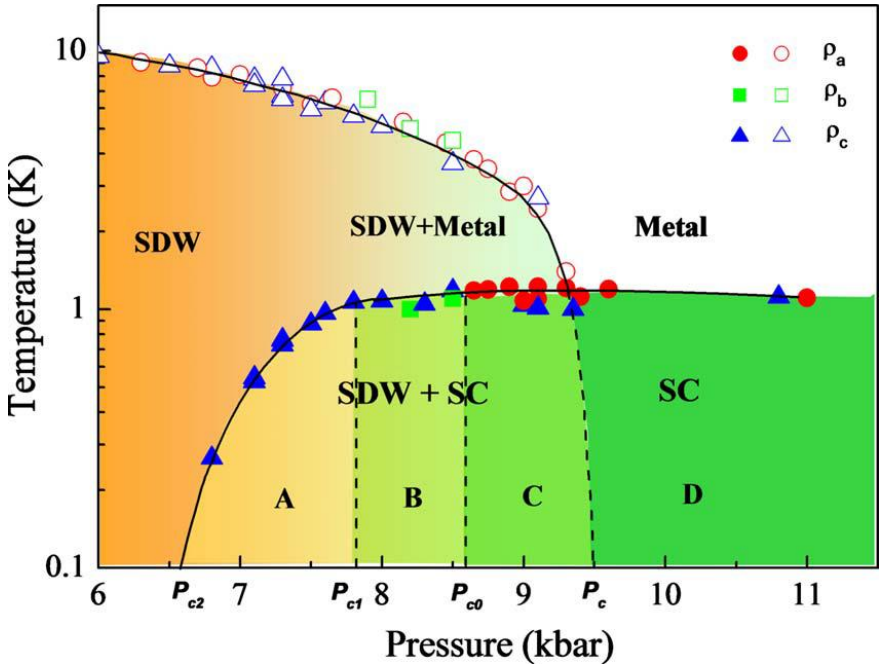

Coexistence of Spin Density Waves and Superconductivity in $(TMTSF)_2PF_6$

Arjun Narayanan,[1,*] Andhika Kiswandhi,[2] David Graf,[2] James Brooks,[2] and Paul Chaikin[1]

AMRO suggest that the coexistence of spin density wave and metal-superconducting orders is neither microscopic nor a soliton wall phase, but a phase separation into domains of the high-pressure metal and the low-pressure spin density wave phases.

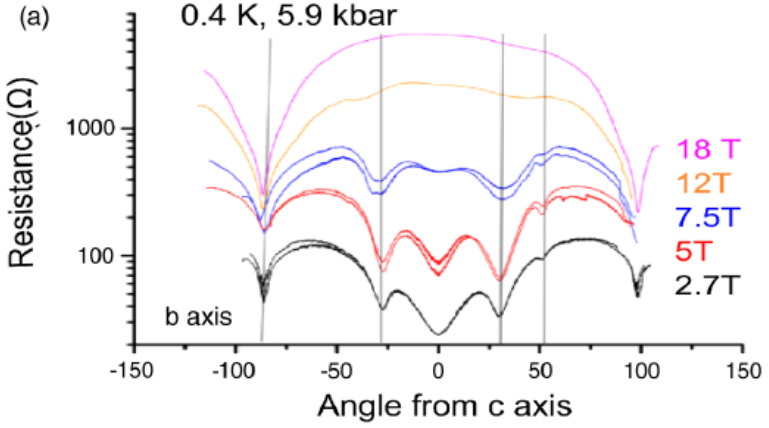

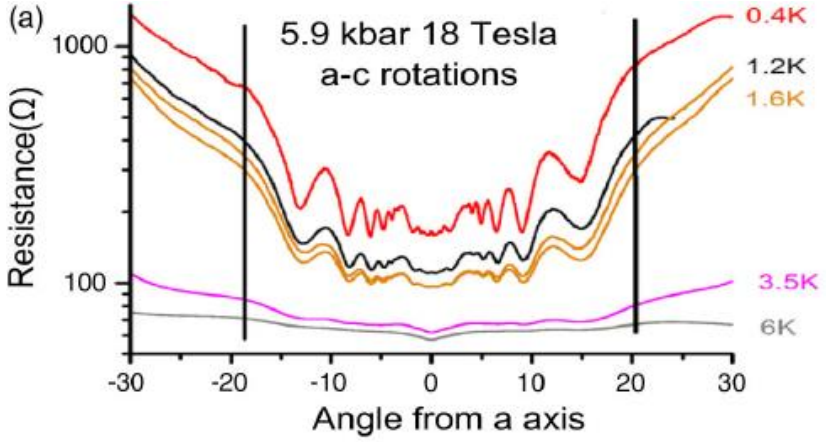

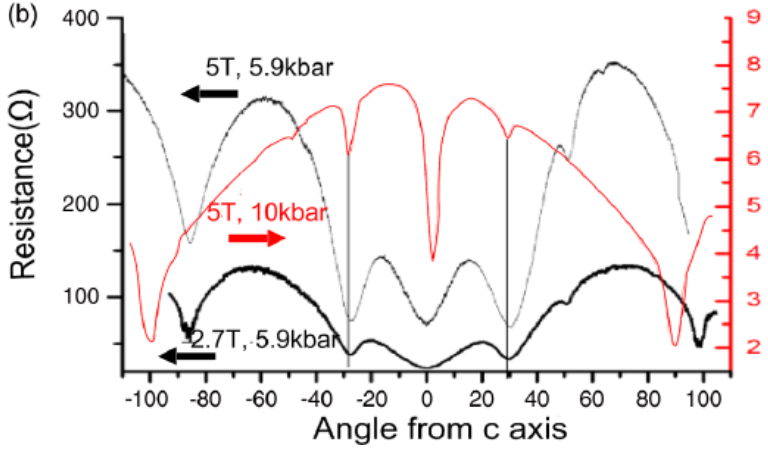

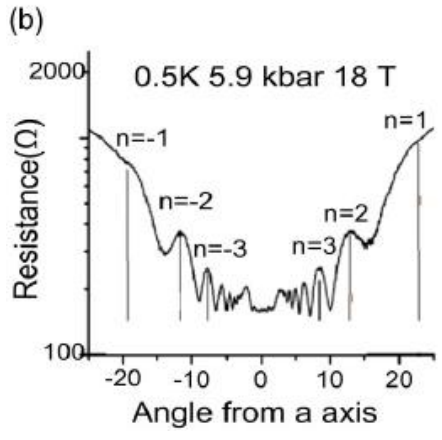

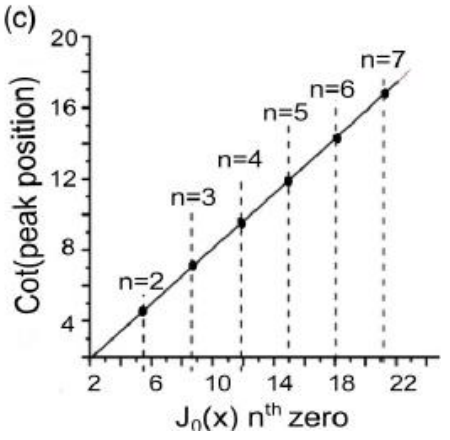

Coexistence of superconductivity and spin-density wave in $(TMTSF)_2ClO_4$: Spatial structure of the two-phase state

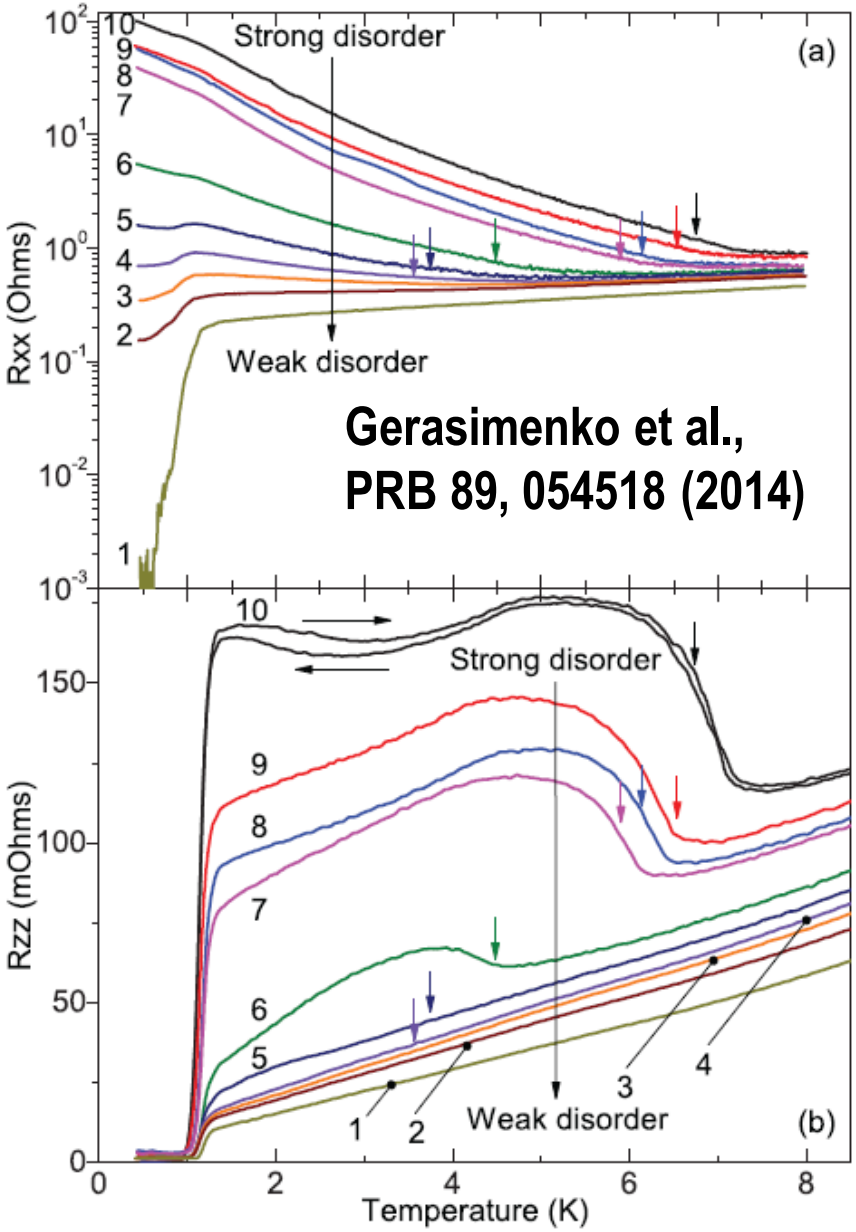

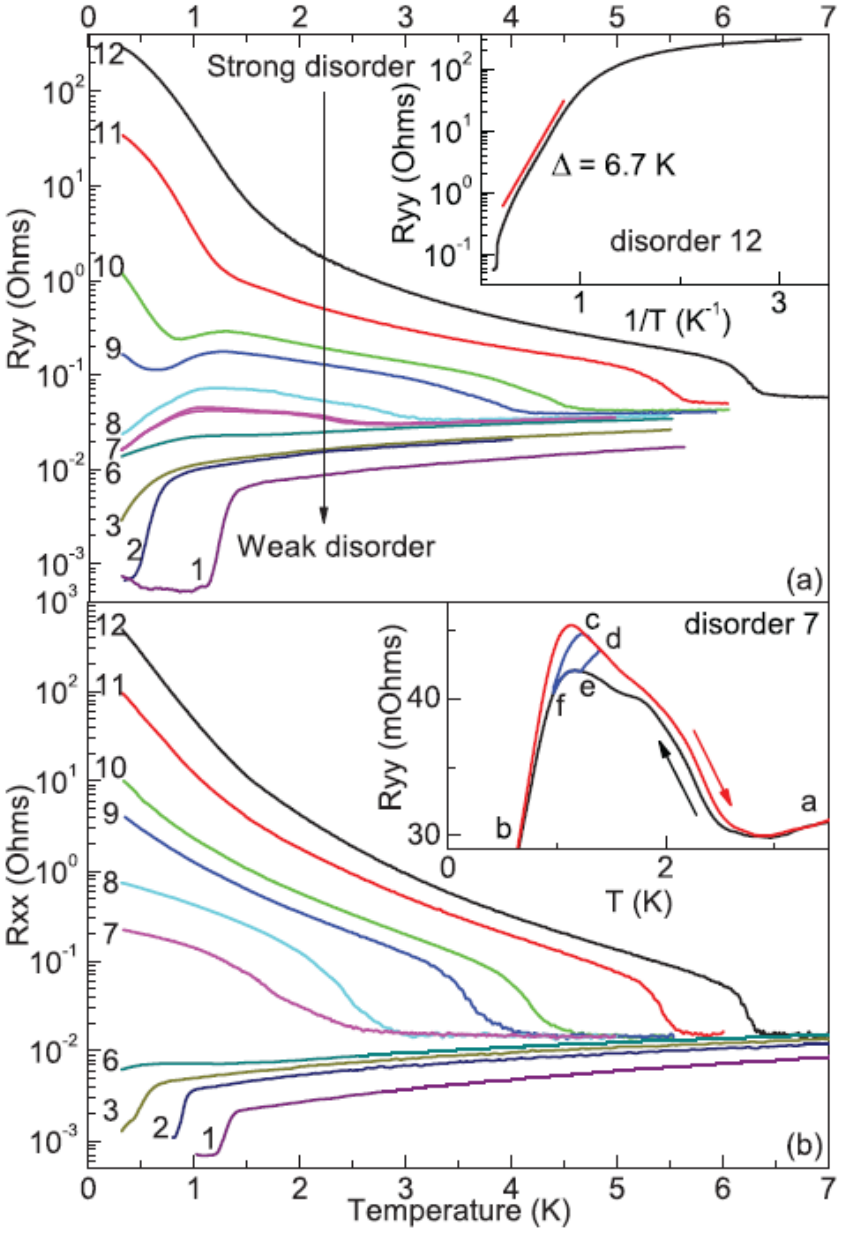

Outlook

Similar behavior in YBCO high-Tc superconductors?

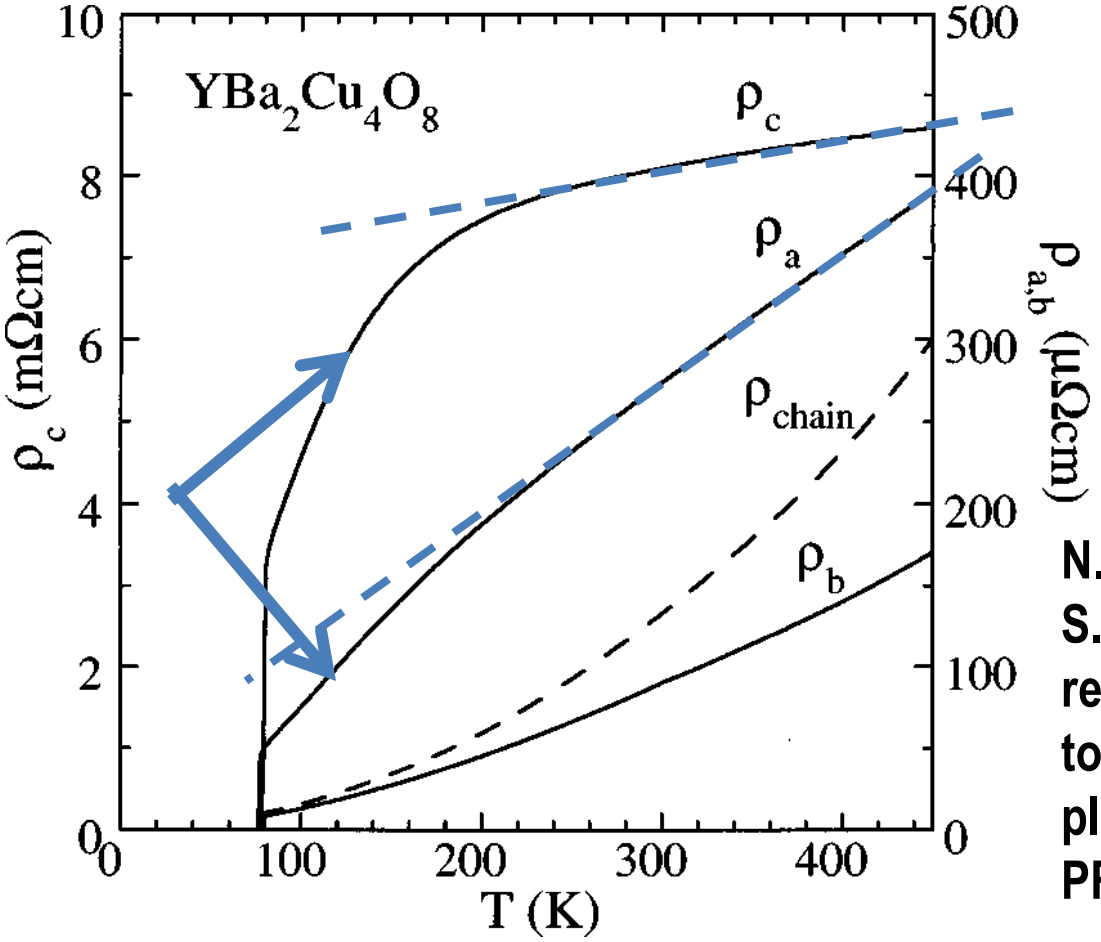

Resistivity along the c-axis (interlayer direction) starts to decrease at T≈250K

N.E.Hussey, K.Nozawa, H.Takagi, S.Adachi and K.Tanabe, "Anisotropic resistivity of $YBa_2Cu_4O_8$: Incoherent-to-metallic crossover in the out-of-plane transport" , PRB 56, R11 423 (1997)

Conclusions

1. A general property is proposed: if superconductivity in anisotropic conductor emerges in the form of isolated superconducting islands, it reduces electric resistivity anisotropically, with maximal effect along the least conducting axis. This gives a simple tool to estimate the volume fraction of superconducting phase, which helps to investigate the onset of high-temperature superconductivity.
2. Using this property and the measurements of electron conductivity and diamagnetism, we show the appearance of inhomogeneous superconductivity (in the form of isolated islands) in a bulk FeSe at ambient pressure and temperature several times higher than Tc = 8K.
3. This property is very simple and general. It may help to detect spatially inhomogeneous superconductivity in other anisotropic compounds, such as cuprates, as $YBa_2Cu_4O_8$, organic metals, etc.
4. The spheroid shape of isolated superconducting islands gives a nice agreement between the temperature dependence of SC volume fraction obtained from the experimental data on diamagnetic response and on electronic transport in bulk FeSe.

Details can be found in A.A. Sinchenko, PG et al., Phys.Rev. B 95,165120 (2017); P. Grigoriev, A.A. Sinchenko et al., JETP Lett. 105 (12), 786 (2017)

Derivation of effective conductivity in the Maxwell's (effective-medium) approximation for heterogeneous media with spherical granules

In the Maxwell's approximation the interaction between rare small granules is neglected, and in the external uniform electric field E_0 each small granule of radius R_i and of conductivity $\sigma_2 \neq \sigma_1$ polarizes and acquires an additional electric dipole moment d_i proportional to its volume and to the strength of field E_0: $\boldsymbol{d}_i = \beta_{12} \boldsymbol{E}_0 R_i^3$,

where $\beta_{12} = (\sigma_2 - \sigma_1) / (\sigma_2 + 2\sigma_1)$ is the "polarizability" of a sphere.

Each such dipole moments changes the electric potential outside the granule by $\Delta\varphi_i = \boldsymbol{d}_i \boldsymbol{r} / r^3$, so that the total change of electric potential far away from the sphere R_0, i.e. at $r \gg R_0$, is given by the sum of all granules inside inhomogeneous sphere of radius R_0, which have total volume fraction ϕ:

$$\Delta\varphi_t = \sum_i \frac{\boldsymbol{d}_i (\boldsymbol{r} - \boldsymbol{r}_i)}{|\boldsymbol{r} - \boldsymbol{r}_i|^3} \approx \frac{\sigma_2 - \sigma_1}{\sigma_2 + 2\sigma_1} \frac{\phi R_0^3}{r^2} E_0; \quad \Delta\varphi_t = \frac{\sigma_e - \sigma_1}{\sigma_e + 2\sigma_1} \frac{R_0^3}{r^2} E_0.$$

On the other hand, a single isotropic sphere of the radius R_0 and effective conductivity σ_e inside a media of conductivity σ_1 in a uniform field E_0 creates an additional potential

Comparing these two results for $\Delta\varphi_t$ gives the equation for the effective conductivity σ_e: $\dfrac{\sigma_e - \sigma_1}{\sigma_e + 2\sigma_1} = \phi \dfrac{\sigma_2 - \sigma_1}{\sigma_2 + 2\sigma_1}$

Derivation of polarization of a spherical granule

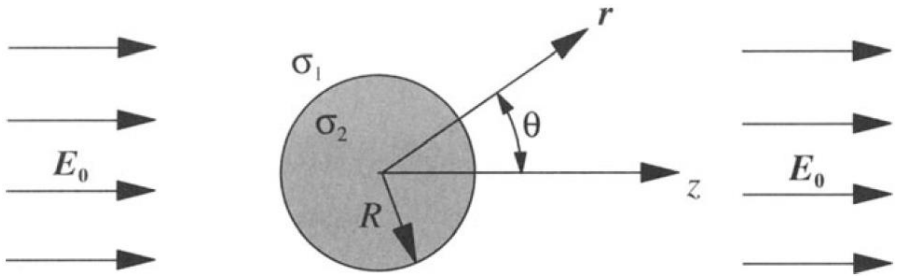

The potential (temperature) field T for a spherical inclusion of radius R and conductivity σ_2 in an infinite matrix of conductivity σ_1 in the applied constant field E_0

satisfies Laplace's equation

$$\Delta T(\boldsymbol{r}) = 0$$

with boundary conditions:

$$T_+ = T_-, \qquad r = R,$$

$$\sigma_1 \boldsymbol{n} \cdot (\nabla T)_+ = \sigma_2 \boldsymbol{n} \cdot (\nabla T)_-, \qquad r = R,$$

$$T = -\boldsymbol{E}_0 \cdot \boldsymbol{r}, \qquad r \to \infty,$$

The solution outside the sphere, i.e. at $r \geq R$,

$$T = -\boldsymbol{E}_0 \cdot \boldsymbol{r} + A\, \boldsymbol{E}_0 \cdot \nabla \left(\frac{1}{r}\right),$$

$$= -E_0 r \cos\theta - A\, E_0 \frac{\cos\theta}{r^2},$$

The solution inside the sphere:

$$T = -\boldsymbol{E}_0 \cdot \boldsymbol{r} + B\, \boldsymbol{E}_0 \cdot \boldsymbol{r}, \qquad r \leq R,$$

$$= -E_0 r \cos\theta + B\, E_0 r \cos\theta,$$

interface continuity conditions give

$$A = -R^3 \frac{\sigma_2 - \sigma_1}{\sigma_2 + 2\sigma_1}, \qquad B = \frac{\sigma_2 - \sigma_1}{\sigma_2 + 2\sigma_1}.$$

$$T = \begin{cases} -\boldsymbol{E}_0 \cdot \boldsymbol{r} + \beta_{21} \boldsymbol{E}_0 \cdot \boldsymbol{r} \left(\dfrac{R}{r}\right)^3, & r \geq R, \\ -\boldsymbol{E}_0 \cdot \boldsymbol{r} + \beta_{21} \boldsymbol{E}_0 \cdot \boldsymbol{r}, & r \leq R, \end{cases}$$

where the "polarizability"

$$\beta_{21} = \frac{\sigma_2 - \sigma_1}{\sigma_2 + 2\sigma_1}.$$

Appendix

Aslamazov-Larkin contribution to conductivity (from SC fluctuations) in layered superconductors

$$\sigma_{xx}^{AL} = \frac{e^2}{16s}\frac{1}{[\epsilon(\epsilon+r)]^{1/2}} \to \frac{e^2}{16s}\begin{cases} 1/\sqrt{\epsilon r}, & \epsilon \ll r \\ 1/\epsilon, & \epsilon \gg r \end{cases}$$

$$\sigma_{zz}^{AL} = \frac{e^2 s}{32\eta_{(2)}}\left(\frac{\epsilon + r/2}{[\epsilon(\epsilon+r)]^{1/2}} - 1\right) \to \frac{e^2 s}{64\eta_{(2)}}\begin{cases} \sqrt{r/\epsilon}, & for \epsilon \ll r \\ (r/2\epsilon)^2, & for \epsilon \gg r \end{cases}$$

where $r = \frac{2\mathcal{J}}{\alpha T} = \frac{4\xi_z^2(0)}{s^2}$, $\epsilon = \ln\frac{T}{T_c} \approx \frac{T - T_c}{T_c} \ll 1$, *s* – interlayer distance.

Contributions from DoS fluctuations

$$\sigma_{\alpha\beta}^{DOS} = -\frac{e^2}{2s}\kappa(T\tau)A_{\alpha\beta}\ln\left(\frac{2}{\epsilon^{1/2} + (\epsilon + r)^{1/2}}\right), \quad \text{where}$$

$$\kappa(T\tau) = \kappa_1 + \kappa_2 = \frac{-\psi'\left(\frac{1}{2} + \frac{1}{4\pi\tau T}\right) + \frac{1}{2\pi\tau T}\psi''\left(\frac{1}{2}\right)}{\pi^2\left[\psi\left(\frac{1}{2} + \frac{1}{4\pi\tau T}\right) - \psi\left(\frac{1}{2}\right) - \frac{1}{4\pi\tau T}\psi'\left(\frac{1}{2}\right)\right]}$$

$$\to \begin{cases} 56\zeta(3)/\pi^4 \approx 0.691, & T\tau \ll 1 \\ 8\pi^2 (T\tau)^2 / [7\zeta(3)] \approx 9.384 (T\tau)^2, & 1 \ll T\tau \ll 1/\sqrt{\epsilon} \end{cases}$$

and $A_{xx} = A_{yy} = 1, A_{zz} = (sJ/v_F)^2, A_{\alpha\neq\beta} = 0$

Appendix

Maki-Thompson contribution

Regular part of the in-plane MT contribution

$$\sigma_{xx}^{MT(reg)} = -\frac{e^2}{2s}\tilde{\kappa}\ln\left(\frac{2}{\epsilon^{1/2}+(\epsilon+r)^{1/2}}\right)$$

where $\tilde{\kappa}(T\tau) = \dfrac{-\psi'\left(\frac{1}{2}+\frac{1}{4\pi\tau T}\right)+\psi'\left(\frac{1}{2}\right)+\frac{1}{4\pi T\tau}\psi''\left(\frac{1}{2}\right)}{\pi^2\left[\psi\left(\frac{1}{2}+\frac{1}{4\pi\tau T}\right)-\psi\left(\frac{1}{2}\right)-\frac{1}{4\pi\tau T}\psi'\left(\frac{1}{2}\right)\right]}$

$$\rightarrow \begin{cases} 28\zeta(3)/\pi^4 \approx 0.346, \ for T\tau \ll 1 \\ \pi^2/\left[14\zeta(3)\right] \approx 0586, \ for 1 \ll T\tau \ll 1/\sqrt{\epsilon} \end{cases}$$

Anomalous part of the in-plane MT contribution

$$\sigma_{xx}^{MT(an)} = \frac{e^2}{4s(\epsilon-\gamma_\varphi)}\ln\left(\frac{\epsilon^{1/2}+(\epsilon+r)^{1/2}}{\gamma_\varphi^{1/2}+(\gamma_\varphi+r)^{1/2}}\right)$$

where, in accordance with [7], the infra-red divergence for the purely 2D case ($r=0$) is cut off at $Dq^2 \sim 1/\tau_\varphi$[1]. The dimensionless parameter

$$\gamma_\varphi = \frac{2\eta}{v_F^2\tau\tau_\varphi} \rightarrow \frac{\pi}{8T\tau_\varphi}\begin{cases} 1, \ T\tau \ll 1 \\ 7\zeta(3)/\left(2\pi^3 T\tau\right), \ 1 \ll T\tau \ll 1/\sqrt{\epsilon} \end{cases}$$

Regular part of the out-of-plane MT contribution is small:

$$\sigma_{zz}^{MT(\mathrm{reg})} = -\frac{e^2 sr\tilde{\kappa}(T\tau)}{16\eta_{(2)}}\left(\frac{(\epsilon+r)^{1/2}-\epsilon^{1/2}}{r^{1/2}}\right)^2$$

Anomalous part of the out-of--plane MT contribution

$$\sigma_{zz}^{MT(\mathrm{an})} = \frac{e^2 s}{16\eta_{(2)}}\left(\frac{\gamma_\varphi+r+\epsilon}{[\epsilon(\epsilon+r)]^{1/2}+[\gamma_\varphi(\gamma_\varphi+r)]^{1/2}}-1\right) \rightarrow \frac{e^2 s}{16\eta_{(2)}}\begin{cases} \sqrt{r/\gamma_\varphi}, \ \epsilon \ll \gamma_\varphi \ll r \\ \sqrt{r/\epsilon}, \ \gamma_\varphi \ll \epsilon \ll r \\ r/(2\epsilon), \ \gamma_\varphi \ll r \ll \epsilon \end{cases}$$